Linear oscillations and stability of a liquid bridge in an axial electric field

N. A. Pelekasis, K. Economou, and J. A. Tsamopoulos[a)]
Laboratory of Computational Fluid Dynamics, Department of Chemical Engineering, University of Patras, Patras 26500, Greece

(Received 14 June 2000; accepted 7 August 2001)

Small amplitude oscillations of viscous, capillary bridges are studied in the presence of an electric dc field. The electric field is proposed as a means to maintain bridges longer than their perimeter and of uniform cylindrical shape. This is desired in the fabrication of semiconductor crystals. The material of the bridge and the surrounding medium is modeled either as a perfect or as a leaky dielectric. The frequency and the damping rate of the oscillations are calculated numerically by solving a generalized eigenvalue problem. It is shown that they depend on the ratios of the dielectric constants, $\epsilon = \epsilon_{in}/\epsilon_{out}$, and conductivities, $S = \sigma_{in}/\sigma_{out}$, of the two materials, the aspect ratio of the bridge, $\Lambda = \pi\tilde{R}/\tilde{L}$, the ratio of viscous to the capillary force, $\mathrm{Oh} = \mathrm{Re}^{-1}$, which can also be viewed as the inverse Reynolds number of the flow, and, finally, the electrical Bond number, C_{el}, which is the ratio of the electric stresses to the capillary force. The stability limit of an initially cylindrical bridge is determined with respect to varicose disturbances. In agreement with previous studies it is shown that, if both materials are perfect dielectrics, application of an electric field has a stabilizing effect on the bridge, in the sense that the minimum value, Λ_{min}, of the aspect ratio for the bridge to remain stable drops below 0.5, irrespective of the specific value of the ratio ϵ. If both materials are leaky dielectrics, bridge stability is determined by the sign of $(S-\epsilon)$ and $(S-1)(\epsilon-1)$, with the positive sign indicating bridge stabilization. The factor $(S-\epsilon)$ arises due to the appearance of a tangential electric stress in the perturbed state for leaky dielectrics. For both cases of leaky and perfect dielectrics, the most unstable mode is the one leading to amphora shaped bridges. It was also found that, when application of an electric field stabilizes the bridge, leaky dielectrics require a lower field than perfect dielectrics and that a large enough field tends to stabilize the bridge for almost the entire range of values of the aspect ratio Λ. These findings concur with earlier analytical results for the stability of jets in longitudinal electric fields and, in conjunction with certain experimental observations, point to the usefulness of the leaky dielectric model pertaining to the stability of bridges. [DOI: 10.1063/1.1416183]

I. INTRODUCTION

A significant amount of research has been recently devoted to the dynamics of liquid bridges, mostly because they find extensive use in the fabrication of single semiconductor crystals of high purity from the melt via the floating zone method.[1] In a different context, a floating zone has been proposed as a convenient system for simultaneously measuring surface tension and viscosity of ceramic materials which melt at high temperatures (1000–3000 °C).[2,3] In the former application resistive heating is used to form a molten bridge between a melting polycrystalline feed rod and a solidified cylindrical crystal. In order to enhance the efficiency and feasibility of the process large bridges with large length to diameter ratios are desired. However, liquid bridges of cylindrical shape are known to become unstable in the presence of capillary and gravitational forces and to be susceptible to buoyancy driven convection. These effects are reduced in space, where, however, a liquid bridge is susceptible to *g*-jitter, spacecraft maneuvers, etc., that may excite oscillations on its free surface. Therefore it is important to know its natural frequencies and decay rates in the presence of such disturbances. More recently, liquid bridges have been used as a means to measure the extensional viscosity of polymeric fluids.[4]

There has been continued interest in the behavior of liquid jets under the influence or not of an electric or gravitational field, because of the numerous industrial applications, such as in ink jet printers, paint spraying, fuel atomization, electrohydrodynamic mixing, etc. The loss of stability of a long column of liquid placed between two solid surfaces and in the presence or absence of a gravitational field was first considered by Plateau.[5] In particular, using hydrostatic theory he found that liquid columns lose their cylindrical shape due to capillarity, provided that the wavelength of the deformation is larger than their circumference. Rayleigh[6] extended Plateau's work using hydrodynamic theory of linear stability and established that masses of cylindrical shape become unstable when the ratio of their length, $\tilde{L}$, to radius, $\tilde{R}$, exceeds 2π. When gravity is present, Coriell, Hardy, and Cordes[7] showed that the minimum aspect ratio, $\Lambda = \pi\tilde{R}/\tilde{L}$, for a liquid bridge to remain stable is increased from 0.5, the value in the absence of gravity, as the density mismatch between the fluid in the bridge and the surrounding medium

a)Author to whom correspondence should be addressed. Fax: +3061-993-255; electronic mail: tsamo@chemeng.upatras.gr

increases. The latter is characterized by the gravitational Bond number, $\mathrm{Bo}=(\Delta\rho g\tilde{R}^2)/\gamma$ identifying the relative magnitude between gravitational and surface tension forces; g is the gravitational acceleration, γ denotes the interfacial tension between the liquid column and the surrounding medium, and $\Delta\rho$ the density difference between the two media. More recently, the results of the hydrostatic analysis for the effect of the Bond number on liquid bridge stability obtained by Coriell *et al.* were reproduced and extended by Tsamopoulos, Chen, and Borkar[8] in the context of hydrodynamic normal mode analysis in the presence of infinitesimal disturbances. Thus they were able to account for viscous effects in the liquid column in order to obtain the frequencies and damping rates of the bridge.

The stabilizing effect of strong electric fields that are aligned with the axis of the fluid cylinder was first pointed out by Raco[9] and Taylor.[10] In this fashion cylindrical jets with aspect ratios Λ as low as 0.06 were observed. In the early distinction of materials to perfect conductors or perfect insulators, Melcher and Taylor[11] added the idea of a leaky dielectric in order to explain certain paradoxical phenomena pertaining to, presumably, nonconducting fluids (Alan and Mason[12]). These phenomena, first explained by Taylor,[13] do not arise in either perfect dielectrics or conductors.[14] A complete characterization of a leaky material as far as its electrical properties are concerned requires both its dielectric constant and its conductivity. The success of this idea and the earlier experiments with jets motivated Saville[15] to examine the linear electrohydrodynamic stability of an infinite fluid cylinder immersed in a longitudinal electric field. Both fluids were treated as leaky dielectrics. This allows for the appearance of interfacial electric charges in a slightly perturbed jet which generate a net shearing force along the interface, in addition to the normal forces that arise as a result of the difference in dielectric constants between the two fluids. These induced shearing electrical stresses must be balanced by mechanical (viscous) stresses, which set an otherwise static fluid in motion. In this fashion he found that a leaky dielectric requires much lower field strength than a perfect dielectric for jet stabilization to take place. In addition he showed that the stability of the cylindrical configuration depends on the relative magnitude of the conductivity and dielectric constant ratios, $\sigma_{\mathrm{in}}/\sigma_{\mathrm{out}}$, $\epsilon_{\mathrm{in}}/\epsilon_{\mathrm{out}}$, between the inner and outer fluid. In the present study it will be seen that such conditions hold in the case of liquid bridges as well. Finally, he pointed out the importance of the viscous boundary layers that form on either side of the interface between the two fluids, on the amplification and damping rates of the two fluid system, when their viscosities are relatively low.

Gonzalez *et al.*[16] conducted a hydrostatic analysis on the stability of a liquid bridge of finite length in zero gravity treating the two fluids as perfect dielectrics. Starting from the cylindrical shape as the basic state, they constructed a bifurcation diagram relating the values of the bridge aspect ratio, the dimensionless field strength, and the dielectric constant ratio. Thus they computed the point where instability first settles giving rise to an antisymmetric shape, to be referred to as amphora shape hereafter, with respect to the central plane dividing the region between the two plates of the bridge, yet axisymmetric. In particular, they showed that the electric field always stabilizes a liquid bridge irrespective of the ratio of dielectric constants between the bridge and its surroundings. They also carried out an experimental investigation of the stability of a liquid bridge in a neutrally buoyant environment using an axial ac electric field. Monitoring the break-up of the bridge with varying electric field intensity, they were able to confirm their theoretical results, especially for large values of the latter, albeit for a single value of $\epsilon=1.8$. They attributed the increasing discrepancy between their experimental and theoretical findings to the more pronounced effect of gravity as the field strength is diminished. Subsequently, Ramos *et al.*[17] extended the previous theory to account for gravitational effects and showed improved agreement with experiments, again for a single case with $\epsilon=1.7$. Still, the predicted electric field, which is required for stabilization of a certain bridge was quite higher than the one measured elsewhere.[18]

At about the same time, Sankaran and Saville[18] examined experimentally the stability of a liquid bridge in a neutrally buoyant environment using an axial dc electric field. Their results confirm the superiority of the leaky dielectric model over the perfect dielectric one, indicating gain or loss of stability with the application of an electric field depending on the conductivities and dielectric constants of the two media as predicted earlier[15] by linear stability analysis. In the following sections it is shown that such an inversion of stability characteristics as a result of interchanging the inner and outer bridge fluids can be explained in the context of leaky dielectric behavior. Finally, they pointed out the difference between the critical field strength for which the basic cylindrical shape of the bridge loses stability to amphora shapes and the field strength required for pinch-off of the bridge to take place. The clear appearance of fluid motion internal and external to the bridge after departure from the static cylindrical shape was achieved, is analogous to the recirculation observed in a drop of leaky dielectric placed in an electric field.[12] It leads to the conclusion that a stability analysis of this problem based on hydrostatics alone may produce results of limited validity. Recent experiments aboard the space shuttle[19] on the stability of liquid bridges subject to an axial electric field confirmed previous terrestrial findings[18] with isopycnic systems while pointing out certain patterns in the dynamics of liquid bridges that do not conform with leaky dielectric behavior; for example, the bulging of the amphora always occurred nearer the positive electrode of the bridge even though the sense of deformation should be independent of field orientation.

The present study is a hydrodynamical approach to liquid bridge stability that accounts for liquid motion, in the perturbed state, inside the bridge. This motion is generated by the interfacial electric stresses, which are shown to arise whether the two fluids are treated as perfect or leaky dielectrics. However, only in the latter case will free electric charge appear at the interface. Pinning the ends of the bridge at the disk surfaces provides a cutoff in the wavelengths allowed in a free jet and makes impossible the analytical solution of the eigenvalue problem.[8] The detailed nonlinear formulation of

the dynamical problem is given in Sec. II, neglecting motion in the surrounding medium and focusing on the cylindrical basic state. However, extension of the same formulation can be used for the examination of different basic states, e.g., those that due to gravity have amphora shapes and, because of this, internal fluid motion due to the electric stresses. This is left for future investigation. The linear limit of infinitesimal disturbances is examined next and the governing differential equations of the eigenvalue problem that determines bridge stability are developed, Sec. III. Due to the finite size of the bridge and the effect of internal fluid motion the problem is best tackled numerically. Thus the finite element method is used for the discretization of the governing equations inside the two fluids. The resulting set of algebraic equations provides the eigenvalues of the two-fluid system as a function of the parameters of the problem: the Ohnesorge number, $\mathrm{Oh}=\mu/(\rho\gamma\tilde{R})^{1/2}$, which can also be viewed as an inverse Reynolds number of the flow, albeit based only on the properties of the bridge fluid (ρ, μ signify its density and viscosity, and γ the interfacial tension), that measures the relative magnitude of viscous and capillary forces, the bridge aspect ratio, $\Lambda=\pi\tilde{R}/\tilde{L}$, the ratio between the two dielectric constants, $\epsilon=\epsilon_{\mathrm{in}}/\epsilon_{\mathrm{out}}$, the ratio between the conductivities of the two fluids, $S=\sigma_{\mathrm{in}}/\sigma_{\mathrm{out}}$ and the dimensionless electric field strength, $C_{el}=(\tilde{\epsilon}_{\mathrm{out}}E_0^2\tilde{R})/\gamma$ (E_0 signifies the magnitude of the axially applied electric field). The numerical solution is outlined in Sec. IV. This procedure is slightly modified in Secs. IV A and IV B in order to capture eigenvalues corresponding to normal modes that are symmetric and antisymmetric, respectively, with respect to the mid-plane defined by the two plates of the bridge. This essentially reduces the computational cost by one-half of the original due to the reduction in the computational domain. In Sec. V A a detailed account of the results of the numerical eigenvalue calculation is presented in terms of the frequencies and the amplification/damping rates of the bridge. The stability limit of the bridge is also given, as this is described by the minimum value of the aspect ratio, Λ_{min}, required for the cylindrical bridge to remain stable, and its variation with the problem parameters, in Sec. V B. It will be seen that some important findings regarding the stability of jets, treated as leaky dielectrics, in the presence of a longitudinal electric field[15] persist in the case of liquid bridges. In addition, general trends of leaky dielectric behavior observed experimentally are reproduced. Finally, in Sec. VI the numerical results are discussed and explained in view of the physics of the problem and conclusions are drawn.

II. GOVERNING EQUATIONS

We are interested in examining the stability of a liquid bridge that is formed by placing liquid between two stationary, cylindrical and coaxial rods which are at a distance $\tilde{L}$ from each other. In the absence of gravity and of an electric field the bridge takes the shape of a perfect cylinder as long as the Plateau stability limit is not exceeded, i.e., $\tilde{L}<2\pi\tilde{R}$, where $\tilde{R}$ is the radius of the circular contact line that the liquid bridge forms as it wets the two planar surfaces; Fig. 1. It is well known that capillary forces sustain the cylindrical

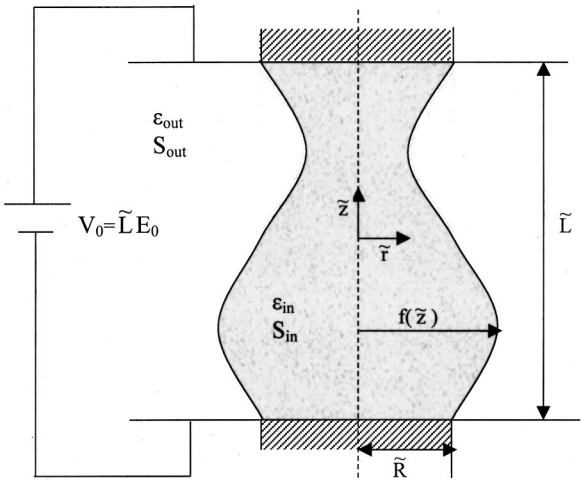

FIG. 1. Schematic diagram of a liquid bridge immersed in a dc electric field.

shape. Although the radius of each rod, $\tilde{R}_r$, is significantly larger than the radius of the contact line, it is assumed that the latter remains fixed, especially under the small bridge perturbations that we consider in this work. Nevertheless, in practice, one can place at each contact area of the rods o-rings or a disk of suitable material with very small but sufficient thickness to prevent spreading of the liquid on the rest of the rod's surface. As a result, the contact line is forced to remain fixed even for larger disturbances.[16,18] A dc electric field is applied between the two rods as a means for studying its effect on bridge stability. Bulk properties of the liquid (density, ρ, viscosity, μ, dielectric constant, ϵ_{in}, and electric conductivity, σ_{in}) as well as interfacial properties (surface tension, γ) are uniform and constant under the present isothermal analysis. In most practical applications the surrounding material is a gas and, thus it is assumed that it has negligible density and viscosity, but uniform and finite dielectric constant, $\tilde{\epsilon}_{\mathrm{out}}$, and electric conductivity, σ_{out}.

Small disturbances may initiate motion of the liquid, which can be easily detected at its interface with the surrounding medium. For axisymmetric bridges, this surface varies with the axial distance and time, $\tilde{f}(\tilde{z},\tilde{t})$. Nonaxisymmetric disturbances are not considered here, since it is known that they manifest themselves at very large field strengths.[10] The physical properties of the liquid and the geometric scales of the bridge affect its motion and stability, as was shown by Tsamopoulos *et al.*[8] in the absence of an electric field. In the latter study the combined effect of gravitational and viscous forces on the stability of a liquid bridge was examined. Here, the research effort is focused on how a dc electric field acting in the axial direction affects both the Plateau stability limit and the frequency and damping rate of the bridge. To this end, the bridge is assumed to oscillate in zero gravity or in a neutrally buoyant environment neglecting any density mismatches between the two fluids. This flow configuration has been realized in various experimental studies, Gonzalez *et al.*,[16] and Sankaran and Saville,[18] among others, and more recently aboard the space shuttle[19] where the effect of buoyancy was practically eliminated. The present investigation focuses on calculating the eigenfrequencies and eigenmodes,

relating them to the physical properties of this system such as the conductivity and dielectric constant ratio, and finally on comparing them against previous theoretical[15,16] and experimental findings.[17–19] The usual cylindrical coordinate system (r,θ,z) is used, which is taken to be coaxial with the two rods with its origin located midway between them.

In the following, the full nonlinear formulation is given describing the dynamics of a liquid bridge that is surrounded by a passive fluid. The formulation allows for treatment of the two fluids as either perfect or leaky dielectrics. First the conservation equations of mass and momentum for the liquid in the bridge are written in dimensionless form:

$$\underline{\nabla}\cdot\underline{v}=0, \tag{1}$$

$$\left(\frac{\partial \underline{v}}{\partial t}+\underline{v}\cdot\underline{\nabla v}\right)=-\underline{\nabla}P+\mathrm{Oh}\,\underline{\nabla}\cdot\underline{\tau}_m, \tag{2}$$

where the velocity components in cylindrical coordinates are $\underline{v}=(u,v,w)$ and the stress tensor due to viscous forces is defined by Newton's law, $\underline{\tau}_m=[\underline{\nabla v}+(\underline{\nabla v})^T]$. As will be seen in the following, the relaxation time for the electric charge in the bulk of the fluids is much smaller than the bridge oscillation time. This prevents any free charge from appearing in the bulk of the liquid and, thus no electric stresses arise in Eq. (2).[11] Variables have been rendered dimensionless with respect to their dimensional counterparts as follows:

$$z=\tilde{z}\frac{\pi}{\tilde{L}},\quad r=\frac{\tilde{r}}{\tilde{R}},\quad P=\tilde{P}\frac{\tilde{R}}{\gamma},$$
$$\underline{v}=\tilde{\underline{v}}\left(\frac{\rho\tilde{R}}{\gamma}\right)^{1/2},\quad t=\tilde{t}\left(\frac{\gamma}{\rho\tilde{R}^3}\right)^{1/2}, \tag{3}$$

with tildes denoting dimensional quantities. Since there is no characteristic velocity in this problem, only physical and geometrical properties appear in the dimensionless number that arises in the momentum balance, Eq. (2), the Ohnesorge number, $\mathrm{Oh}=\mu/(\rho\gamma\tilde{R})^{1/2}$. Alternatively, the inverse Oh can be viewed as a modified Reynolds number of the flow. Different length scales have been used in the radial and axial directions and their ratio, $\Lambda=\pi\tilde{R}/\tilde{L}$, is the second dimensionless parameter of this system. It arises, for example, in the dimensionless form of the gradient operator:

$$\underline{\nabla}=\underline{e}_r\frac{\partial}{\partial r}+\underline{e}_\theta\frac{1}{r}\frac{\partial}{\partial\theta}+\underline{e}_z\Lambda\frac{\partial}{\partial z}. \tag{4}$$

The usual no-slip and no-penetration boundary conditions apply at both solid surfaces,

$$\underline{v}(r,z=\pm\tfrac{1}{2})=\underline{0}. \tag{5}$$

We will take the azimuthal velocity to be zero throughout the bridge. Also, since we will be considering only axisymmetric disturbances, the radial velocity and the radial derivative of the axial velocity are zero at the centerline,

$$u=\frac{\partial w}{\partial r}=0,\quad r=0. \tag{6}$$

In the interfacial force balances that primarily govern the deformation and motion of the free surface, electric stresses will necessarily arise. Their determination requires the calculation of the electric field in both the bridge and the surrounding medium. At this point it should be stressed that both media are taken to be charge free, since their respective charge relaxation times,[10–12] $\tilde{\epsilon}_{\mathrm{in}}/\sigma_{\mathrm{in}}$, $\tilde{\epsilon}_{\mathrm{out}}/\sigma_{\mathrm{out}}$, are much smaller than the characteristic time for bridge oscillations (bridge radius up to 1 cm) which is scaled via $(\tilde{R}^3\rho/\gamma)^{1/2}$. Therefore, Gauss' law for a charge-free medium that is linearly polarizable and uniform, irrespective of being perfect or leaky dielectric, reduces to calculating the electric potential in either phase by solving Laplace's equation:

$$\nabla^2V^{\mathrm{in,out}}=0, \tag{7}$$

where the electric field, charge and potential are made dimensionless by a characteristic field, E_0:

$$\tilde{\underline{E}}=E_0\underline{E},\quad \tilde{Q}=(\tilde{\epsilon}_{\mathrm{out}}E_0)Q,\quad \tilde{V}=\left(E_0\frac{\tilde{L}}{\pi}\right)V,$$
$$\tilde{\underline{E}}=\underline{\nabla}\tilde{V},\quad \underline{E}=\frac{1}{\Lambda}\underline{\nabla}V; \tag{8}$$

$\tilde{\epsilon}_{\mathrm{in}}=\epsilon_{\mathrm{in}}\tilde{\epsilon}_0$, $\tilde{\epsilon}_{\mathrm{out}}=\epsilon_{\mathrm{out}}\tilde{\epsilon}_0$ correspond to the permittivities of the inner and outer fluids, respectively, with $\tilde{\epsilon}_0=8.85\times10^{-12}$ (in MKS units) denoting the permittivity of free space. The boundary conditions associated with the imposed field set the electric potential to be constant along each rod/fluid interface extending all the way to the dimensionless radius of the rods, $\tilde{R}_r/\tilde{R}$:

$$V^{\mathrm{in,out}}(r,\pm\pi/2)=\pm\pi/2,\quad 0\leqslant r\leqslant\tilde{R}_r/\tilde{R} \tag{9}$$

and enforce symmetry at the common axis of the rods and field uniformity far away from the bridge:

$$\frac{\partial V^{\mathrm{in}}}{\partial r}(r=0,z)=0, \tag{10a}$$

$$\lim_{r\to\infty}\frac{\partial V^{\mathrm{out}}}{\partial r}(r,z)\to0. \tag{10b}$$

In most experiments the radius of the two rods, $\tilde{R}_r$, is about 10 times as large as the bridge radius, $\tilde{R}$, and this has been shown to allow for neglecting end effects in the electric field at their edges.[10,16]

The boundary conditions on the fluid/fluid interface depend on whether the materials are assumed to be perfect or leaky dielectrics.[11,20] If both fluids are assumed to be perfect dielectrics, they do not carry any electric charge even at their common interface and they do not allow any current to pass through this interface, where Gauss' law again holds:

$$\epsilon\underline{n}\cdot\underline{E}^{\mathrm{in}}=\underline{n}\cdot\underline{E}^{\mathrm{out}}\quad\text{at } r=f(z,t), \tag{11}$$

where $\epsilon=\epsilon_{\mathrm{in}}/\epsilon_{\mathrm{out}}$. If both fluids are assumed to be leaky dielectrics, surface charge will arise at their common interface. Then, the conservation law of surface charge (Eq. II in Melcher and Taylor[11]) equates the rate of its accumulation on the interface to (i) the net flux of charge to the interface from either phase, (ii) the net rate of addition due to surface cur-

rent, and (iii) the net rate of charge overtake due to the translation of the interface along its normal. Thus the interfacial charge conservation equation reads

$$t_r\frac{\partial Q}{\partial t}=S\underline{n}\cdot\underline{E}^{\text{in}}-\underline{n}\cdot\underline{E}^{\text{out}}-S\nabla_\Sigma\underline{K}+t_r\underline{n}\cdot\underline{v}(\rho_{e,\text{out}}-\rho_{e,\text{in}})$$

$$\text{at } r=f(z,t), \tag{12}$$

where $S=\sigma_{\text{in}}/\sigma_{\text{out}}$, ∇_Σ is the surface divergence, and $\underline{K}$ represents the surface current density which includes contributions due to convection and conduction of surface charge,[11] $\rho_{e,\text{in}}$ and $\rho_{e,\text{out}}$ represent charge density in the bulk of the two fluids, and t_r is the ratio of charge relaxation time to the characteristic time for bridge oscillation:

$$t_r=\frac{(\tilde{\epsilon}_{\text{out}}/\sigma_{\text{out}})}{(\rho\tilde{R}/\gamma)^{1/2}}. \tag{13}$$

As mentioned already, for materials of interest (insulators and imperfect conductors) and typical bridge diameters, $t_r\to 0$, whereas t_r becomes large for conducting materials. In order to be consistent with the assumption of immediate charge equilibration in the bulk of the fluid we will take $t_r=0$. In this case, the net surface charge can be calculated *a posteriori* from Gauss' law:

$$Q=\epsilon\underline{n}\cdot\underline{E}^{\text{in}}-\underline{n}\cdot\underline{E}^{\text{out}} \quad \text{at } r=f(z,t). \tag{14}$$

Of course, for both perfect and leaky dielectrics, the irrotationality of the electric field reduces at the interfaces to requiring that its tangential component be continuous or, equivalently, that the electric potential be continuous there:

$$\underline{t}\cdot\underline{E}^{\text{in}}=\underline{t}\cdot\underline{E}^{\text{out}} \text{ or } V^{\text{in}}=V^{\text{out}} \quad \text{at } r=f(z,t). \tag{15}$$

Given the values of parameters, S, and ϵ, Eqs. (7)–(15) are sufficient to determine the electric field in both fluids, if their common interface is known. The latter is determined by the interfacial stress balance and the kinematic condition. The total (mechanical and electrical) tangential stress must be zero and the total normal stress must be balanced by the capillary force. This is compactly written as

$$\left[-P\underline{\underline{I}}+(\text{Oh}\,\underline{\underline{\tau}}_m+\epsilon C_{el}\underline{\underline{\tau}}_e^{\text{in}}-C_{el}\underline{\underline{\tau}}_e^{\text{out}})\right]\cdot\underline{n}+2H\underline{n}=\underline{0}$$

$$\text{at } r=f(z,t). \tag{16}$$

The pressure in the outer fluid has been set to zero. In Eq. (16), C_{el} is the dimensionless electrical Bond number, which is the ratio of the electric to the surface tension forces and is defined as

$$C_{el}=\frac{\tilde{\epsilon}_{\text{out}}E_0^2\tilde{R}}{\gamma}. \tag{17}$$

The permittivity of the medium surrounding the bridge is used in the above definition in accordance with previous experimental studies.[18] In all the above equations $\underline{n}$ and $\underline{t}$ are the unit normal and tangent vectors on the free interface, respectively. According to the Mongé representation, every point on the interface may be described by the position vector $\underline{F}(z,t)=f(z,t)\underline{e}_r+(z/\Lambda)\underline{e}_z$ and as a result vectors $\underline{n}$ and $\underline{t}$ are given by

$$\underline{n}=\frac{\underline{e}_r-\Lambda f_z\underline{e}_z}{D^{1/2}}, \tag{18}$$

$$\underline{t}=\frac{\Lambda f_z\underline{e}_r+\underline{e}_z}{D^{1/2}}, \tag{19}$$

where $D=1+\Lambda^2 f_z^2$ and subscript z denotes partial differentiation with respect to that coordinate. For an incompressible and uniform material, the electric stress tensor is defined (Stratton[21]) by

$$\underline{\underline{\tau}}_e=\underline{E}\underline{E}-\tfrac{1}{2}|\underline{E}|^2\underline{\underline{I}} \text{ with } \tilde{\underline{\underline{\tau}}}_e=\underline{\underline{\tau}}_e\tilde{\epsilon}_0E_0^2, \tag{20}$$

where $|\underline{E}|$ is the magnitude of $\underline{E}$. The curvature of the free interface, has been made dimensionless by $\tilde{R}^{-1}$ and it is given by

$$-2H=\frac{1+\Lambda^2(f_z^2-ff_{zz})}{(1+\Lambda^2f_z^2)^{3/2}}\frac{1}{f}. \tag{21}$$

The final boundary condition on the moving surface is the kinematic condition that equates the velocity of the surface to the liquid velocity there:

$$\underline{n}\cdot\frac{\partial\underline{F}}{\partial t}=\underline{n}\cdot\underline{v} \quad \text{at } r=f(z,t). \tag{22}$$

Throughout the motion, the line of contact of the liquid/gas interface with each cylindrical rod remains fixed at the edge of each original contact surface. According to the analysis by Benjamin and Scott,[22] this is the relevant condition, especially when a sharp corner is present in the supporting solid surface. Thus

$$f(t)=1, \quad z=\pm\tfrac{1}{2}\pi. \tag{23}$$

Finally, the volume of the liquid bridge must remain constant during the motion. Although other cases may be readily examined, the volume is taken here to be that of a perfect cylinder spanning the distance between the rods:

$$V\equiv\frac{\tilde{V}}{\tilde{R}^2\tilde{L}}=\frac{1}{2\pi}\int_0^{2\pi}\int_{-\pi/2}^{\pi/2}f^2\,dz\,d\theta=\pi. \tag{24}$$

III. BASIC STATE AND THE EIGENVALUE PROBLEM

In order to calculate the eigenvalues and eigenmodes of this system all equations will be linearized around a steady state. To this end, small and volume-preserving disturbances will be assumed for all dependent variables. Thus the dynamic state of the system is described, in the limit of infinitesimal disturbances of amplitude $\delta\ll 1$, as

$$\begin{bmatrix}\underline{v}\\P\\f\\\underline{\underline{\tau}}_m\\\underline{\underline{\tau}}_e\\V\\Q\end{bmatrix}=\begin{bmatrix}\underline{v}_b\\P_b\\f_b\\\underline{\underline{\tau}}_{mb}\\\underline{\underline{\tau}}_{eb}\\V_b\\Q_b\end{bmatrix}+\delta\begin{bmatrix}\underline{v}_p\\P_p\\f_p\\\underline{\underline{\tau}}_{mp}\\\underline{\underline{\tau}}_{ep}\\V_p\\Q_p\end{bmatrix}, \tag{25}$$

where subscript b indicates the base state and the subscript p the perturbed one. When gravitational effects are negligible the base state corresponds to a static cylindrical shape. Then,

$2H_b=1$, $\underline{n}_b=\underline{e}_r$, and $\underline{t}_b=\underline{e}_z$. Therefore, the electric field in both fluids is aligned with the axial direction and Eq. (11) or (14) indicate that no charge is accumulated on the fluid/fluid interface and no tangential electric stresses arise, whether a perfect or a leaky dielectric model is used, respectively. In other words the electric field has no effect on a bridge of perfect cylindrical shape. Thus

$$\begin{bmatrix} \underline{v}_b \\ P_b \\ f_b \\ \underline{\underline{\tau}}_{mb} \\ \underline{\underline{\tau}}_{eb} \\ V_b \\ Q_b \end{bmatrix} = \begin{bmatrix} \underline{0} \\ 1-C_{el}(\epsilon-1)/2 \\ 1 \\ \underline{0} \\ -\frac{1}{2}\begin{bmatrix} 1 & 0 & 0 \\ 0 & 1 & 0 \\ 0 & 0 & -1 \end{bmatrix} \\ z \\ 0 \end{bmatrix}. \tag{26}$$

It is noteworthy that the base pressure is modified from the one in the absence of electric field by a factor that is proportional to the difference in dielectric constants of the two fluids, $\epsilon-1$. As ϵ is raised above unity the base pressure in the bridge decreases, compared to the value it would have attained in the absence of the electric field.

Introducing Eqs. (25) and (26) into the governing equations of the previous section results in a set of linear equations in terms of the perturbed variables. The equations describing the hydrodynamic aspects of the flow are

$$\underline{\nabla}\cdot\underline{v}_p=0, \tag{27}$$

$$\frac{\partial \underline{v}_p}{\partial t}=-\underline{\nabla}P_p+\mathrm{Oh}\,\underline{\nabla}\cdot\underline{\underline{\tau}}_{mp}, \tag{28}$$

$$\underline{v}_p(r,z=\pm\tfrac{1}{2}\pi)=0, \tag{29}$$

$$u_p=\frac{\partial w_p}{\partial r}=0, \quad r=0. \tag{30}$$

The linearized equations for the calculation of the electrical field are

$$\nabla^2 V_p^{\mathrm{in,out}}=0, \tag{31}$$

$$V_p^{\mathrm{in,out}}(r,\pm\pi/2)=0, \quad 0\leqslant r\leqslant \tilde{R}_r/\tilde{R}, \tag{32}$$

$$\frac{\partial V_p^{\mathrm{in}}}{\partial r}(r=0,z)=0, \tag{33a}$$

$$\lim_{r\to\infty}\frac{\partial V_p^{\mathrm{out}}}{\partial r}(r,z)\to 0, \tag{33b}$$

$$V_p^{\mathrm{in}}=V_p^{\mathrm{out}} \quad \text{at } r=f_b, \tag{34}$$

with the following condition for a perfect dielectric, resulting from Eq. (11):

$$\epsilon\frac{\partial V_p^{\mathrm{in}}}{\partial r}-\frac{\partial V_p^{\mathrm{out}}}{\partial r}=\Lambda^2\frac{\partial f_p}{\partial z}(\epsilon-1) \quad \text{at } r=f_b, \tag{35}$$

or with the following two conditions for a leaky dielectric, resulting from Eqs. (12) and (14), respectively:

$$S\frac{\partial V_p^{\mathrm{in}}}{\partial r}-\frac{\partial V_p^{\mathrm{out}}}{\partial r}=\Lambda^2\frac{\partial f_p}{\partial z}(S-1) \quad \text{at } r=f_b, \tag{36}$$

and

$$Q_p=(\epsilon-S)\left(\frac{\partial V_p^{\mathrm{in}}}{\partial r}-\Lambda^2\frac{\partial f_p}{\partial z}\right) \quad \text{at } r=f_b. \tag{37}$$

Equations (35) and (36) constitute the linearized form of the interfacial condition for the electric field pertaining to the cylindrical bridge situation at base state, which is the one considered here. The last equation can be used *a posteriori*, i.e., after the solution of the linear problem, in order to calculate the induced surface charge. It should be pointed out that, as can be seen from Eq. (37) the surface charge is obtained as the product of $(S-\epsilon)$ and the normal component of the perturbed field evaluated on the side of the bridge fluid. Consequently the surface charge vanishes when $S=\epsilon$, as is the case with perfect dielectrics. In the following we use this condition, $S=\epsilon$, in order to identify perfect dielectrics and it will be seen that deviations from it will play an essential role in the stability of leaky dielectrics.

The linearized equations for the interfacial force balance, the kinematic condition, and the condition that fixes the two contact lines read

$$[-P_p\underline{\underline{I}}+(\mathrm{Oh}\,\underline{\underline{\tau}}_{mp}+\epsilon C_{el}\underline{\underline{\tau}}_{ep}^{\mathrm{in}}-C_{el}\underline{\underline{\tau}}_{ep}^{\mathrm{out}})]\cdot\underline{n}_b+2H_p\underline{n}_b$$
$$+[-P_b\underline{\underline{I}}+2H_b+\epsilon C_{el}\underline{\underline{\tau}}_{eb}^{\mathrm{in}}-C_{el}\underline{\underline{\tau}}_{eb}^{\mathrm{out}}]\cdot\underline{n}_p=0, \quad r=f_b, \tag{38}$$

$$\underline{n}_b\cdot\underline{e}_r\frac{\partial f_p}{\partial t}=\underline{n}_b\cdot\underline{v}_p, \quad r=f_b, \tag{39}$$

$$f_p(t,z=\pm\tfrac{1}{2}\pi)=0, \tag{40}$$

where $\underline{n}_p=-\Lambda(\partial f_p/\partial z)\underline{e}_z$ denotes the perturbed normal vector at the interface and $2H_p$ is the linearly perturbed surface curvature:

$$2H_p=-f_p-\Lambda^2\frac{\partial^2 f_p}{\partial z^2}. \tag{41}$$

It can be easily shown by applying the divergence theorem on the linearized continuity equation (27) in conjunction with the kinematic condition (39), that the linearized volume conservation is automatically satisfied by any linear disturbance that initially preserves the bridge volume. Thus volume conservation need not be imposed as an additional independent condition that has to be satisfied by the bridge. Finally, according to the standard methodology, all perturbed variables are expressed as

$$\begin{bmatrix} u_p(r,z,t) \\ w_p(r,z,t) \\ V_p(r,z,t) \\ P_p(r,z,t) \\ f_p(z,t) \\ \underline{\underline{\tau}}_{e,p}(r,z,t) \\ Q_p(t) \end{bmatrix} = \begin{bmatrix} \overline{u}(r,z) \\ \overline{w}(r,z) \\ \overline{V}(r,z) \\ \overline{P}(r,z) \\ \overline{f}(z) \\ \overline{\underline{\underline{\tau}}}_e(r,z) \\ \overline{Q} \end{bmatrix} e^{-\sigma t}, \tag{42}$$

where σ is an eigenvalue of the system and it is complex in general, $\sigma=\sigma_r+i\sigma_i$. After introducing Eq. (42) into the equations for the perturbed variables, an equation set is obtained that is similar to the one given above, except for the substitution for the time derivatives: $\partial(\,)/\partial t\rightarrow-\sigma(\,)$.

Typically, a distinct eigenvalue corresponds to each eigenmode. If the real part of all eigenvalues is positive, the base state is linearly stable and the distinct values of σ_r and σ_i correspond to the damping rate and frequency of each mode, respectively. On the other hand, if the real part of even one eigenvalue is negative the system is unstable. Clearly the values of σ depend on the parameters of the system $(\mathrm{Oh},\Lambda,C_{el},\epsilon,S)$. Points in the parameter space at which $\sigma_r=0$ are identified as bifurcation points from the perfect cylindrical shape. It should also be noted that, if needed, the methodology followed in this section can be used in order to study the stability of more complicated basic states, namely those pertaining to ''amphora'' shapes induced by gravity and entailing internal motion of the fluid. Clearly then, the details of the initial bridge configuration will be different from those given in Eq. (26). Such an examination is not pursued here and is left for a future study.

IV. NUMERICAL SOLUTION

Equations (27)–(41) will be reduced to an algebraic generalized eigenvalue problem for the eigenvalues, σ, and the corresponding eigenvectors. To this end, the finite-element method is employed. The radial and axial velocity components as well as the electric potential, the perturbed pressure, and the perturbed shape are represented by biquadratic Lagrangian functions, $\Phi_i(r,z)$, bilinear Lagrangian functions, $X_i(r,z)$, and quadratic Lagrangian functions $\Omega_i(z)$, respectively:

$$\begin{bmatrix}\overline{u}\\ \overline{w}\\ \overline{V}\end{bmatrix}(r,z)=\sum_{i=1}^{N}\begin{bmatrix}u_i\\ w_i\\ V_i\end{bmatrix}\Phi_i(r,z),$$
$$\overline{P}(r,z)=\sum_{i=1}^{M}p_iX_i(r,z),\quad \overline{f}(z)=\sum_{i=1}^{L}f_i\Omega_i(z), \tag{43}$$

where L, M, and N are the number of coefficients in each summation. Galerkin's procedure is employed in order to construct the residual equations. Equation (27) is multiplied by the trial function X_i, Eqs. (28) and (31) are multiplied by the trial function Φ_i, and Eq. (39) is multiplied by the trial function Ω_i. Subsequently, they are integrated over the respective domain. Integration by parts or the divergence theorem are applied, where necessary, in order to reduce second-order derivatives to first-order ones. Thus the weak form of the governing equations is obtained:

$$R_{Ci}=\int_A X_i\underline{\nabla}\cdot\overline{\underline{v}}\,q\,dA, \tag{44}$$

$$\begin{aligned}\underline{R}_{Mi}=&\int_A\left[-\sigma\overline{\underline{v}}+\frac{1}{r}(-\overline{P}+\mathrm{Oh}\,\overline{\tau}_{m\theta\theta})\underline{e}_r\right]\Phi_i\,dA+\int_A\underline{\nabla}\Phi_i\cdot(-\overline{P}\underline{\underline{I}}+\mathrm{Oh}\,\overline{\underline{\tau}}_m)dA\\&+\int_{-\pi/2}^{\pi/2}\Phi_i2\overline{H}\underline{e}_r\,dz+\int_{-\pi/2}^{\pi/2}\Phi_i(-P_b+1)\Lambda\left(-\frac{\partial\overline{f}}{\partial z}\right)\underline{e}_z\,dz+\int_{-\pi/2}^{\pi/2}\Phi_iC_{el}(\epsilon\overline{\underline{\tau}}_{elb}^{\mathrm{in}}-\overline{\underline{\tau}}_{elb}^{\mathrm{out}})|_{r=f_b}\cdot\Lambda\left(-\frac{\partial\overline{f}}{\partial z}\right)\underline{e}_z\,dz\\&+\int_{-\pi/2}^{\pi/2}\Phi_iC_{el}(\epsilon\overline{\underline{\tau}}_{el}^{\mathrm{in}}-\overline{\underline{\tau}}_{el}^{\mathrm{out}})|_{r=f_b}\cdot\underline{e}_r\,dz-\int_0^1\underline{e}_r\overline{\tau}_{mrz}\Phi_i|_{z=-\pi/2}^{z=\pi/2}r\,dr+\int_0^1\underline{e}_z(\overline{P}-\overline{\tau}_{mzz})\Phi_i|_{z=-\pi/2}^{z=\pi/2}r\,dr,\end{aligned} \tag{45}$$

$$\begin{aligned}R_{Ei}^{\mathrm{in,out}}=&-\int_A\left(\frac{\partial\Phi_i}{\partial r}\frac{\partial\overline{V}^{\mathrm{in,out}}}{\partial r}+\Lambda^2\frac{\partial\Phi_i}{\partial z}\frac{\partial\overline{V}^{\mathrm{in,out}}}{\partial z}\right)dA\\&\pm\int_{-\pi/2}^{\pi/2}\Phi_ir\left.\frac{\partial\overline{V}^{\mathrm{in,out}}}{\partial r}\right|_{r=f_b}dz\\&+\int_0^1\Phi_i\left.\frac{\partial\overline{V}^{\mathrm{in,out}}}{\partial z}\right|_{z=-\pi/2}^{z=\pi/2}r\,dr,\end{aligned} \tag{46}$$

$$R_{Ki}=\int_{-\pi/2}^{\pi/2}\Omega_i(-\sigma\overline{f}-\overline{u})dz. \tag{47}$$

The residuals, R_{ci}, $\underline{R}_{Mi}$, R_{Ei}, and R_{Ki} correspond to continuity, momentum, electric potential, and kinematic equations. In these general expressions $dA=r\,dr\,dz$, $0\leqslant r\leqslant f_b=1$, $-\pi/2\leqslant z\leqslant\pi/2$, and $2H_p=2\overline{H}e^{-\sigma t}$. Boundary conditions (30) and (38) have been incorporated in Eq. (45) and Eqs. (33a), (33b) have been incorporated in Eq. (46). It is the coupling through the interfacial balances at $r=f_b$ that brings about the influence of the electric field on bridge oscillations and stability. In Eq. (45), if we concentrate on the interfacial terms and ignore, for the moment, the contribution due to the disturbance in the curvature then the line integrals involving interaction between the base state and the correction to the normal vector at the interface due to the disturbance, $\Lambda(\partial\overline{f}/\partial z)\underline{e}_z$, along with the line integral involving interaction between the perturbed electric stresses and the base normal vector, $\underline{e}_r$, give

$$\int_{-\pi/2}^{\pi/2}\Phi_i(-P_b+1)\Lambda\left(-\frac{\partial\overline{f}}{\partial z}\right)\underline{e}_z\,dz + \int_{-\pi/2}^{\pi/2}\Phi_i C_{el}(\epsilon\underline{\underline{\tau}}_{elb}^{\text{in}}-\underline{\underline{\tau}}_{elb}^{\text{out}})|_{r=f_b}\cdot\Lambda\left(-\frac{\partial\overline{f}}{\partial z}\right)\underline{e}_z\,dz + \int_{-\pi/2}^{\pi/2}\Phi_i C_{el}(\epsilon\overline{\underline{\underline{\tau}}}_{el}^{\text{in}}-\overline{\underline{\underline{\tau}}}_{el}^{\text{out}})|_{r=f_b}\cdot\underline{e}_r\,dz = \int_{-\pi/2}^{\pi/2}\Phi_i C_{el}\left[\frac{\partial\overline{V}^{\text{in}}}{\partial z}(1-\epsilon)\underline{e}_r\right]_{r=f_b}dz \tag{48}$$

for a perfect dielectric ($S=\epsilon$), whereas for a leaky dielectric they read

$$\int_{-\pi/2}^{\pi/2}\Phi_i(-P_b+1)\Lambda\left(-\frac{\partial\overline{f}}{\partial z}\right)\underline{e}_z\,dz + \int_{-\pi/2}^{\pi/2}\Phi_i C_{el}(\epsilon\underline{\underline{\tau}}_{elb}^{\text{in}}-\underline{\underline{\tau}}_{elb}^{\text{out}})|_{r=f_b}\cdot\Lambda\left(-\frac{\partial\overline{f}}{\partial z}\right)\underline{e}_z d + \int_{-\pi/2}^{\pi/2}\Phi_i C_{el}(\epsilon\overline{\underline{\underline{\tau}}}_{el}^{\text{in}}-\overline{\underline{\underline{\tau}}}_{el}^{\text{out}})|_{r=f_b}\cdot\underline{e}_r\,dz = \int_{-\pi/2}^{\pi/2}\Phi_i C_{el}\left[\frac{\partial\overline{V}^{\text{in}}}{\partial z}(1-\epsilon)\underline{e}_r+(\epsilon-S)\times\left(\frac{1}{\Lambda}\frac{\partial\overline{V}^{\text{in}}}{\partial r}-\Lambda\frac{\partial\overline{f}}{\partial z}\right)\underline{e}_z\right]_{r=f_b}dz. \tag{49}$$

The rest of the essential conditions will be dealt with in the next subsections. At this point it is important to note that in the case of perfect dielectrics, $S=\epsilon$, the only surviving stress component on the perturbed surface is the normal one. When leaky dielectrics are considered both normal and tangential electric stresses are acting on the two fluid interface, as a result of the perturbed electric field. This feature of leaky dielectrics was also pointed out by Saville[15] in the context of jet electrohydrodynamic stability and will be seen to play an essential part in the determination of the stability characteristics of a liquid bridge also.

In Eq. (46) the plus and minus signs in front of the line integral at $r=f_b$ correspond to the inner and outer fluids, respectively. In general, a different electric potential is defined in the inner and the outer fluid. However, continuity of potentials at the fluid/fluid interface, Eq. (34), eliminates the outer potential there, for example, and one may treat the electric potential as a single variable in both fluids. On the other hand, this variable must have a discontinuous normal derivative at this interface. This discontinuity can be easily incorporated in the finite element formulation, through the line integral at $r=f_b$ in Eq. (46). For a perfect dielectric and for an initially cylindrical bridge, Eq. (35) reduces the contributions to this line integral from the two fluids to

$$\int_{-\pi/2}^{\pi/2}\Phi_i r\left(\frac{\partial\overline{V}^{\text{in}}}{\partial r}-\frac{\partial\overline{V}^{\text{out}}}{\partial r}\right)\Bigg|_{r=f_b}dz = \int_{-\pi/2}^{\pi/2}\Phi_i r\left(\left(\frac{\partial\overline{V}^{\text{in}}}{\partial r}-\Lambda^2\frac{\partial\overline{f}}{\partial z}\right)(1-\epsilon)\right)\Bigg|_{r=f_b}dz. \tag{50}$$

Instead, for a leaky dielectric, use of Eq. (36) reduces the same contributions to

$$\int_{-\pi/2}^{\pi/2}\Phi_i r\left(\frac{\partial\overline{V}^{\text{in}}}{\partial r}-\frac{\partial\overline{V}^{\text{out}}}{\partial r}\right)\Bigg|_{r=f_b}dz = \int_{-\pi/2}^{\pi/2}\Phi_i r\left(\left(\frac{\partial\overline{V}^{\text{in}}}{\partial r}-\Lambda^2\frac{\partial\overline{f}}{\partial z}\right)(1-S)\right)\Bigg|_{r=f_b}dz. \tag{51}$$

In an effort to improve the accuracy of eigenvalue calculations for the case of very large conductivities of the bridge fluid compared with the surrounding medium, $S\to\infty$, as is the case with certain pairs of fluids often used in experimental investigations, e.g., water/air or castor oil-eugenol bridges suspended in silicone oil,[18,19] in Eqs. (49) and (51) we set $S-\epsilon\sim S$ and $S-1\sim S$, respectively, and subsequently we apply the interfacial condition (36) in order to introduce the term

$$\frac{\partial V_p^{\text{out}}}{\partial r}-\Lambda^2\frac{\partial f_p}{\partial z}$$

instead of

$$S\frac{\partial V_p^{\text{in}}}{\partial r}-\Lambda^2\frac{\partial f_p}{\partial z}S,$$

thus eliminating S from the problem formulation while introducing $O(1)$ quantities in the numerical formulation which are easier to approximate.

Equations (43)–(51) constitute a generalized eigenvalue problem of the form

$$\underline{\underline{A}}\,\underline{x}=\sigma\underline{\underline{B}}\,\underline{x}, \tag{52}$$

where $\underline{\underline{A}}$ and $\underline{\underline{B}}$ are coefficient matrices and $\underline{x}$ is the eigenvector corresponding to the eigenvalue σ. An IMSL routine (DGVLRG) may be used in order to calculate all the complex eigenvalues and eigenvectors of the discretized equations for given values of the problem parameters. Owing to the large storage and CPU time requirements associated with calculating all the eigenvalues via the IMSL routine, the Arnoldi method was used which calculates a restricted number of the eigenvalues depending on their magnitude. This approach follows closely the variation of the Arnoldi method as developed by Lehoucq and Scott[23] who have incorporated several improvements in the original Arnoldi algorithm and made it available through the internet. We typically calculated up to 100 eigenvalues with the Arnoldi method. In this fashion the computation of eigenvalues of a (3300×3300) double precision matrix and, when needed, the corresponding eigenvectors required about 50 min in CPU time as opposed to 3.5 h using the standard IMSL routine on a SG Origin 200 that calculates the complete set of eigenvalues. The calculation of the eigenvectors follows the procedure

described in Ref. 8. On the other hand, the computational effort and requirements may be reduced by a factor of 2 or more and the accuracy may be increased by calculating separately the symmetric and antisymmetric modes of the system. In fact, the results of the numerical investigation presented in Sec. V were obtained in this fashion. In the process, proper boundary conditions must be set at $z=0$, so that only half of the domain is discretized ($0\leqslant r\leqslant R_r/R,\ 0\leqslant z\leqslant \pi/2$). These conditions are explained in detail in Secs. IV A and IV B for symmetric and antisymmetric modes, respectively.

The accuracy of the numerical results has been verified by calculating the eigenvalues in the absence of an electric field and comparing them with those calculated by Tsamopoulos *et al.*[8] and with those calculated by Borkar and Tsamopoulos[24] in the limit of very small Oh (large Re) number. Convergence of eigenvalues has been verified by refinement of the mesh in both the *r*- and *z*-directions. Twelve elements were found to be sufficient in the radial direction in each phase, appropriately packed around the fluid/fluid interface. Extending the outer domain to $\tilde{R}_r/\tilde{R}=10$ was found to be sufficient, so that the calculations are not affected by its actual location. A ratio of $\tilde{R}_r/\tilde{R}=80/5$ was used in the experimental investigation of Gonzalez *et al.*[16] whereas the ratio between the diameter of the outer glass containment, four cm, and the diameter of the rings containing the bridge in the apparatus described in Refs. 18, 19, 4.7 mm, is roughly 10. Furthermore, 16 elements are required in the axial direction (in the half of the domain) in order to achieve at least four significant digits of accuracy in the first mode, especially for small values of Oh. Accuracy drops to three significant digits for higher eigenmodes. Finally, it was also found that as Λ approaches zero, accuracy decreases. Therefore, eigenvalues obtained in that limit are reported here up to the computed accuracy.

A. Symmetric modes

Shapes of liquid bridges are symmetric about the midplane of the bridge, $z=0$, when

$$\partial\overline{f}/\partial z=0,\quad z=0. \tag{53}$$

According to the analysis by Tsamopoulos *et al.*[8] the eigenvectors then correspond to the odd modes, so that shapes are described by an infinite summation of cosines. Moreover, the radial component of the velocity must be symmetric and the axial component must be zero at the midplane:

$$\partial\overline{u}/\partial z=\overline{w}=0\quad \text{at}\quad z=0. \tag{54}$$

Using Eqs. (27) and (54) it may also be shown that

$$\overline{\tau}_{mrz}=\partial^2\overline{w}/\partial z^2=0\quad \text{at}\quad z=0. \tag{55}$$

Finally, introducing Eqs. (54) and (55) in the axial component of the momentum balance results in

$$\partial\overline{P}/\partial z=0,\quad z=0. \tag{56}$$

In order to solve in the upper half of the domain the essential conditions at the upper plate, Eq. (29), allow for discarding both momentum balances there altogether. Similarly, at $z=0$ the essential condition (54) allows for discarding the axial momentum balance there. On the other hand, the natural condition (54) at $z=0$ eliminates the line integral involving $\overline{\tau}_{mrz}$ from the radial momentum balance in Eq. (45). Similarly the electric potential is symmetric at the midplane:

$$\partial\overline{V}/\partial z=0,\quad z=0. \tag{57}$$

Therefore, the last line integral at $z=0$ will be discarded from Eq. (46), and this equation will not be written at all at $z=\pi/2$ due to the essential condition, Eq. (32).

B. Antisymmetric modes

Antisymmetric shapes of liquid bridges arise when the interface shape, the radial velocity component, and the electric potential assume the same numerical value, but with opposite sign above and below the mid-plane. For example:

$$\overline{u}\big|_{z=+\Delta z}=-\overline{u}\big|_{z=-\Delta z},\quad z=0. \tag{58}$$

Since all three variables are continuous functions, it follows that

$$\overline{u}=\frac{\partial^n\overline{u}}{\partial r^n}=\overline{V}=\frac{\partial^n\overline{V}}{\partial r^n}=\overline{f}=0\quad \text{at}\quad z=0\quad \text{and for}\quad n=1,2,\ldots. \tag{59}$$

In this case the bridge shape is described by a summation of sines. Due to the essential conditions, Eqs. (59) and (32) on the electric potential at $z=0$, and $\pi/2$, respectively, Eq. (46) will not be written at all at these boundaries. Combining Eqs. (59) and (27) yields

$$\frac{\partial\overline{w}}{\partial z}=\tau_{mzz}=0, \tag{60a}$$

$$z=0. \tag{60b}$$

Also due to Eqs. (58) and (59),

$$\left.\frac{\partial\overline{u}}{\partial z}\right|_{z=+\Delta z}=\left.\frac{\partial\overline{u}}{\partial z}\right|_{z=-\Delta z}, \tag{61}$$

and in the limit of $\Delta z\to 0$,

$$\frac{\partial^2\overline{u}}{\partial z^2}=0,\quad z=0. \tag{62}$$

Substitution of Eqs. (59), (60), and (61) into the radial component of the momentum equation reduces it to $\partial\overline{P}/\partial r(z=0)=0$, which upon integration gives

$$\overline{P}=\text{const},\quad z=0. \tag{63}$$

Without loss of generality, this constant is taken to be equal to zero. Again, in order to solve in the upper half of the domain, the essential conditions at the upper plate, Eq. (29), allow for discarding both of the momentum balances there. Similarly, at $z=0$ the essential condition (59) allows for discarding the radial momentum balance there. On the other hand, natural condition (60b) along with Eq. (62) at $z=0$ eliminate the line integral involving $(\overline{P}-\overline{\tau}_{mzz})$ from the axial momentum balance in Eq. (45).

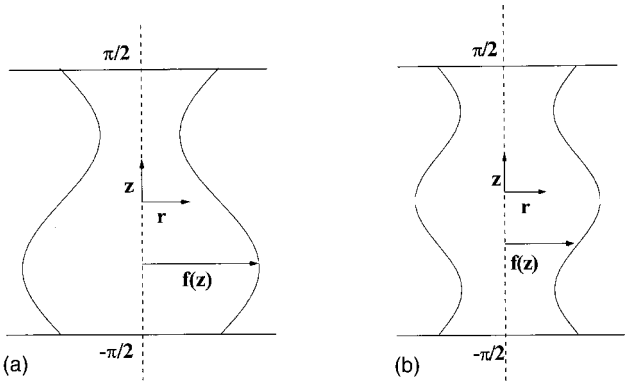

FIG. 2. Schematic representation of the first two axisymmetric eigenmodes; (a) first antisymmetric mode, (b) first symmetric mode.

V. RESULTS AND DISCUSSION

A. Eigenfrequencies and damping/growth rates of the liquid bridge

Using the above described numerical methodology an extensive parametric study was conducted aiming at identifying the dynamic characteristics of a bridge of finite length in the limit of infinitesimally small disturbances. To this end, the real (damping rate, $\sigma_r>0$, or growth rate, $\sigma_r<0$) and imaginary parts (frequency, σ_i) of the first four eigenvalues were monitored. They correspond to the volume preserving varicose eigenmodes with 1, 2, 3, and 4 extrema in the half interval ($0\leqslant z\leqslant \pi/2$), respectively (Fig. 2 shows a schematic representation of the first two modes for the entire bridge). As a first step toward connecting the results of this study with those available in the literature, the effect of $\mathrm{Re}\equiv 1/\mathrm{Oh}$ is examined on the linear dynamics of a bridge characterized by the following dimensionless quantities: $\Lambda=2$, $\epsilon=80$, $S=100$, and $\epsilon C_{el}=0.6$. These are simply taken as representative values chosen in order to exemplify general trends. Situations corresponding to specific pairs of fluids inside and outside the bridge will be considered at the end of this section. Figures 3(a), 3(b) show the dependence of the damping rate and frequency on Oh^{-1}. In general, higher modes correspond to bridges with more distorted shapes which, for this reason, are damped faster. Similarly, surface tension is more effective with disturbancies of smaller wavelength leading to higher frequencies for the higher modes. In the limit as $\mathrm{Oh}^{-1}\rightarrow\infty$ the damping rate of the four modes approaches asymptotically zero as predicted by inviscid theory (Sanz and Diez)[25] and boundary layer theory[24] in the absence of an electric field. As Oh^{-1} becomes smaller, $\mathrm{Oh}^{-1}<5$, viscous damping increases logarithmically, a behavior also observed numerically by Strani and Sabetta[26] for viscous oscillations of free or supported drops. It should also be mentioned that, besides the fact that here $\Lambda>0.5$, the presence of an electric field further stabilizes the already stable bridge, given the particular value for S as will be discussed later. The frequencies of the four modes approach a constant value in the limit of large Oh^{-1}, whereas they decrease sharply as Oh^{-1} becomes smaller than, roughly, 5.0. This effect is more intense for higher eigenmodes. It is anticipated that for some small but finite value of Oh^{-1} the complex eigenvalues will give rise to an overdamped pair of two real positive ones indicating pure damping. Such a trend has also been identified by Tsamopoulos *et al.*,[8] in their study on the stability of liquid bridges when the density mismatch between the interior and exterior fluids is neglected and in the absence of an electric field, and by Strani and Sabetta[26] for viscous drop oscillations.

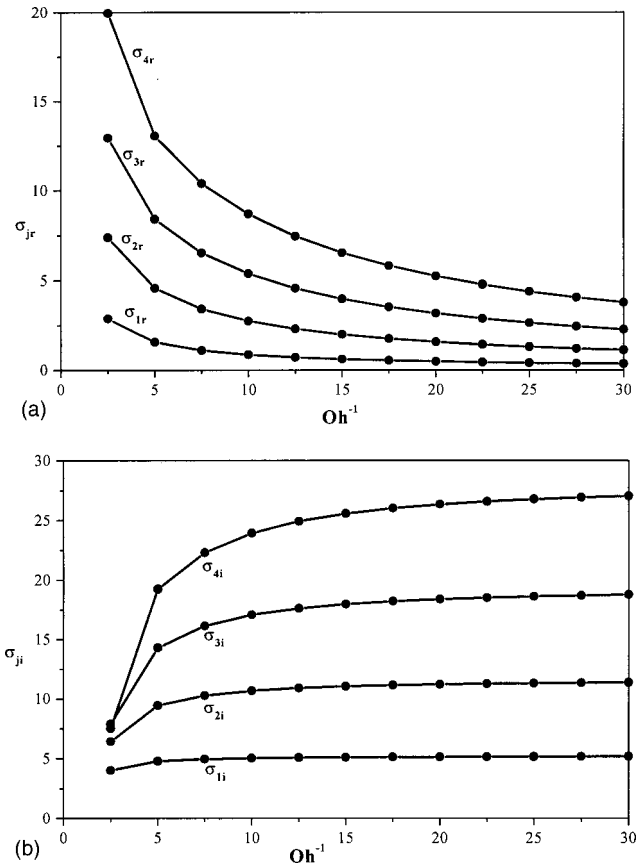

FIG. 3. Evolution of the (a) real and (b) imaginary parts of the eigenvalues corresponding to the first four eigenmodes, $\sigma_{jr} j=1....4$, with increasing Oh^{-1}; $S=100$, $\epsilon=80$, $\Lambda=2$, $C_{el}\epsilon=0.6$.

Figures 4(a), 4(b) show the effect of the electric field intensity, as this is expressed through C_{el}, on the damping rate and oscillation frequency of the bridge; $\Lambda=2$, $\mathrm{Oh}=0.1$, $\epsilon=80$, and $S=100$. The almost linear increase of both σ_r and σ_i with C_{el} indicates the tendency of the field to stabilize the bridge. It will be seen in the following how this behavior is affected by the particular choice of S and ϵ. This monotonic dependence is a consequence of the stretching of the bridge surface induced by the repulsion forces between electric charges that are induced on the fluid/fluid interface due to the field. In addition, the values obtained when the electric field is turned off, $C_{el}=0$, agree very well with those shown in Fig. 2 and Table II in Ref. 8 when the gravitational Bond number is zero. The product $C_{el}\epsilon$ is used here as well as in the following graphs, representing a dimensionless electric field based entirely on properties of the bridge fluid.

The effect of ϵ and S on bridge dynamics is shown in Figs. 5(a), 5(b), 6(a), and 6(b), respectively; in Figs. 5(a), 5(b), $\Lambda=2$, $\mathrm{Oh}=0.1$, $S=20$, and $C_{el}\epsilon=0.6$, whereas in Figs. 6(a), 6(b), $\Lambda=2$, $\mathrm{Oh}=0.1$, $\epsilon=80$, and $C_{el}\epsilon=0.6$. The effect

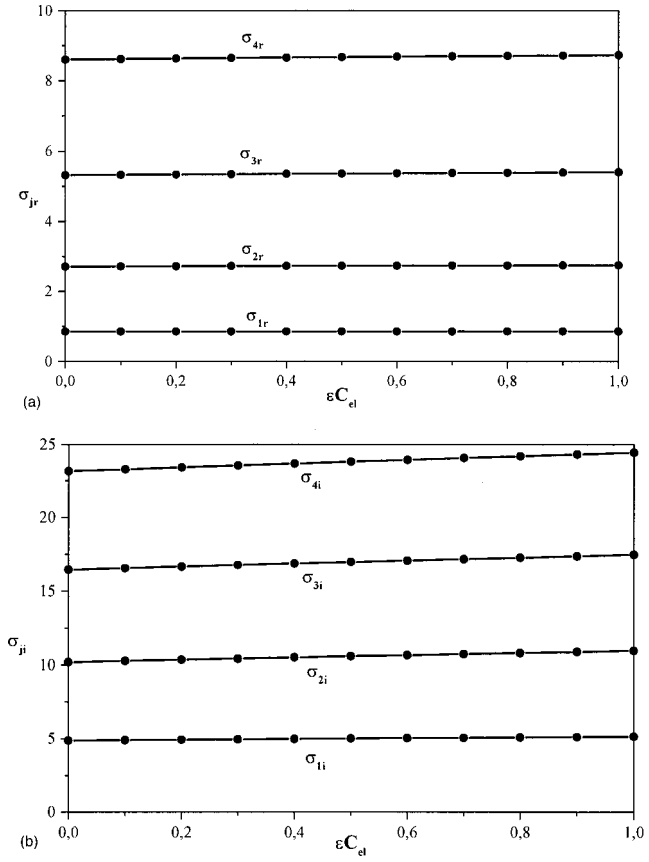

FIG. 4. Evolution of the (a) real and (b) imaginary parts of the eigenvalues corresponding to the first four eigenmodes, $\sigma_{jr} j=1....4$, with increasing $C_{el}\epsilon$; $S=100$, $\epsilon=80$, $\Lambda=2$, Oh$=0.1$.

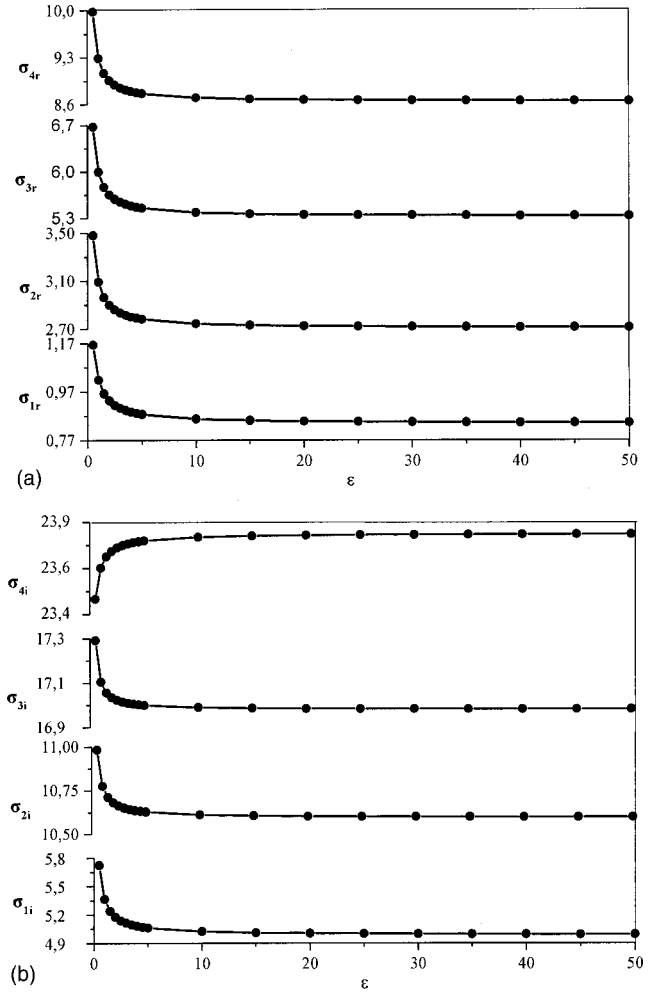

FIG. 5. Evolution of the (a) real and (b) imaginary parts of the eigenvalues corresponding to the first four eigenmodes, $\sigma_{jr} j=1....4$, with increasing ϵ; $S=20$, $C_{el}\epsilon=0.6$, $\Lambda=2$, Oh$=0.1$.

of increasing the permittivity ratio ϵ is to decrease the damping rate, Fig. 5(a), until a constant positive value is reached asymptotically for large values of ϵ. An interesting effect of increasing ϵ is observed in the imaginary part of the eigenvalues, representing the frequency of bridge oscillations, Fig. 5(b). In particular, the frequency of the fourth mode is slightly increasing rather than decreasing as the inner to outer permittivity ratio is increasing. This is probably due to the stronger effect of the normal force on the bridge due to the electric stress [radial component of the force in Eq. (48) or (49)] which intensifies bridge oscillations. Similar is the effect of ϵ on the eigenvalues when $S<1$.

As shown in Figs. 6(a), 6(b), the effect of increasing S is to stabilize the bridge by increasing the damping rate. In fact, as the conductivity ratio acquires large positive values the real part of the eigenvalues increases until it reaches a plateau approaching an asymptotic value in the limit $S\to\infty$ with ϵ constant. A similar behavior is exhibited by the imaginary part. When $S=\epsilon$, the leaky dielectric model reduces to a perfect dielectric one and the eigenvalues obtained by Gonzalez *et al.*[16] are recovered.

The effect of the aspect ratio Λ on bridge stability is shown in Figs. 7(a), 7(b) in terms of the variation of the damping rate and frequency, respectively. The well known fact that a longer bridge, of a cylindrical shape with smaller Λ, is less stable than a shorter one of the same volume when subjected to an axial electric field, is reflected in the decrease of the damping rate for all four modes with decreasing Λ. This is mostly due to the destabilizing effect of surface tension. As a matter of fact, as the aspect ratio Λ is decreased below 0.42 the damping rate of the eigenvalue corresponding to the first asymmetric mode becomes negative indicating instability. For $\Lambda<0.42$ the two complex conjugate eigenvalues of the first mode turn real, one positive and one negative. Only the latter one, indicating instability, is shown in Fig. 7. A similar behavior is exhibited by the first symmetric mode when $\Lambda<0.1$. In fact as Λ further decreases higher asymmetric and symmetric modes become unstable. Evaluation of the exact value of aspect ratio Λ for which such modes become unstable was not pursued since the stability limit of a cylindrical bridge is primarily determined by the first mode and the accuracy of calculations deteriorates when Λ becomes excessively small.

B. Bridge stability

As mentioned above, an important measure of the effect of the applied electric field on bridge stability is the critical value of the aspect ratio, $\Lambda_{\min}$, below which the bridge loses stability to the first varicose mode. An extensive discussion

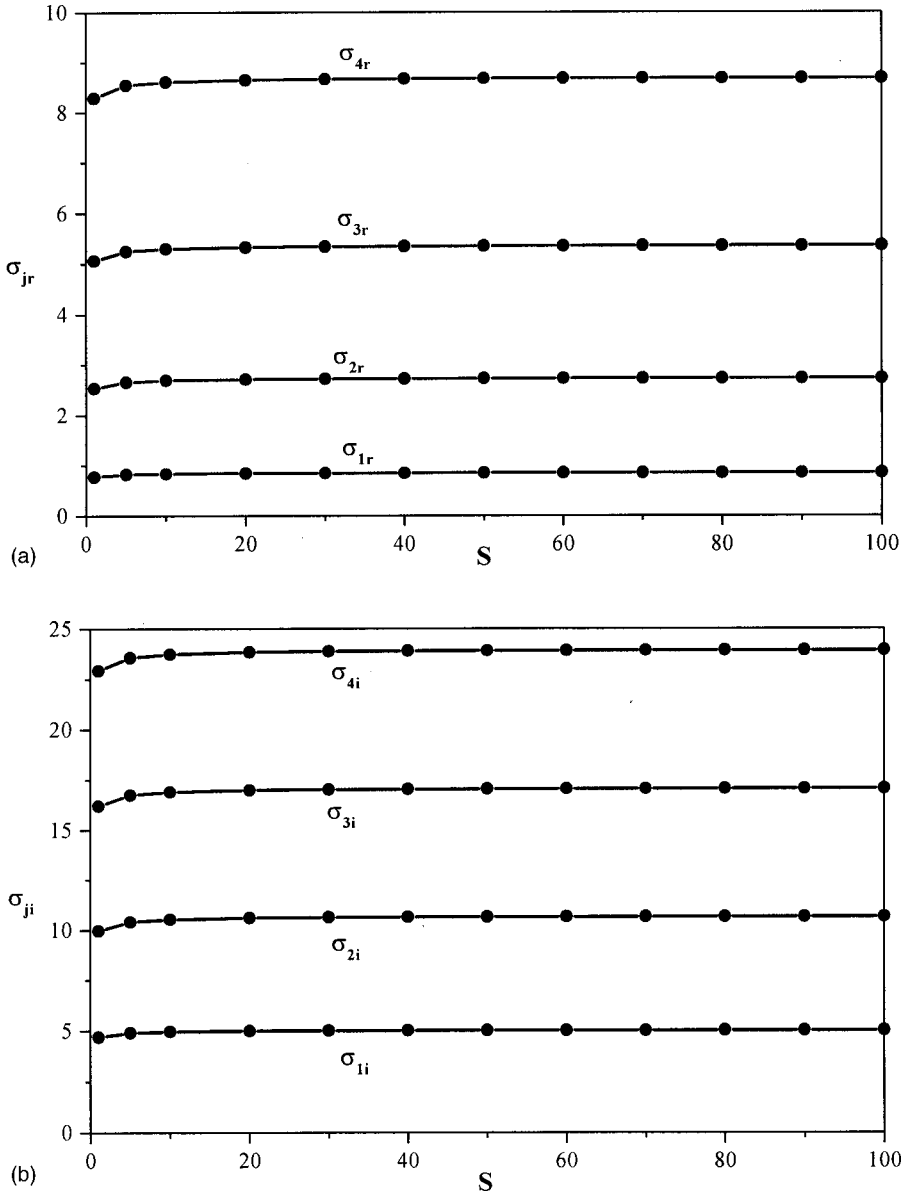

FIG. 6. Evolution of the (a) real and (b) imaginary parts of the eigenvalues corresponding to the first four eigenmodes, $\sigma_{jr} j=1....4$, with increasing S; $C_{el}\epsilon=0.6$, $\epsilon=80$, $\Lambda=2$, Oh$=0.1$.

on the effect of S and ϵ on the stability of a liquid bridge of finite length as well as specific conditions for which application of an axial field can actually be destabilizing, as its intensity increases (increasing C_{el}), are given in the following. A numerical search was conducted on the evolution of $\Lambda_{\min}$ as a function of the problem parameters and it was found that the stabilization or destabilization of the electric bridge, in other words whether the minimum aspect ratio for bridge stability $\Lambda_{\min}$ lies below or above 0.5 which is the value obtained in the absence of the electric field, depends on the factors $(S-\epsilon)$ and $(S-1)(\epsilon-1)$ as suggested by Saville[15] for the case of a cylindrical jet in the presence of an electric field that is aligned with its axis of symmetry. Upon closer examination of Eqs. (48)–(51) it becomes evident that $(S-\epsilon)$ signifies the action of the tangential stress due to the perturbed electric field on the bridge. On the other hand, the factor $(S-1)(\epsilon-1)$ signifies the effect of the normal electric stress on the bridge. This was first pointed out in Ref. 15 for a cylindrical jet, its validity for the case of a bridge is not obvious and will be better demonstrated in Sec. VI. Thus when $(S-\epsilon)>0$ the tangential stress stabilizes the first mode and consequently the bridge, reducing $\Lambda_{\min}$ below 0.5. Similarly, when $S>1$ and $\epsilon>1$ the normal electric stress has a stabilizing effect on the bridge. The opposite happens when $(S-\epsilon)<0$ and $(S-1)(\epsilon-1)<0$. The overall effect of the electric field on the bridge is a result of the combined effect of these two stress components. Figure 8 shows the evolution of $\Lambda_{\min}$ with increasing strength of the axial field, ϵC_{el}, for S ranging between 30 and 0.5, ϵ set to 10 and Oh to 0.1. As S increases from its value corresponding to perfect dielectrics, $S=\epsilon$, application of the field has a stabilizing effect forcing $\Lambda_{\min}$ below 0.5, with $\Lambda_{\min}$ decreasing as the deviation of $S-\epsilon$ from zero grows larger. As soon as $S-\epsilon$ becomes negative the tangential stress has a destabilizing effect, whereas $(S-1)(\epsilon-1)$ is stabilizing as long as S remains above unity. Thus there is a critical value of S between 2 and 9 for which application of the electric field actually destabilizes the bridge and this destabilization be-

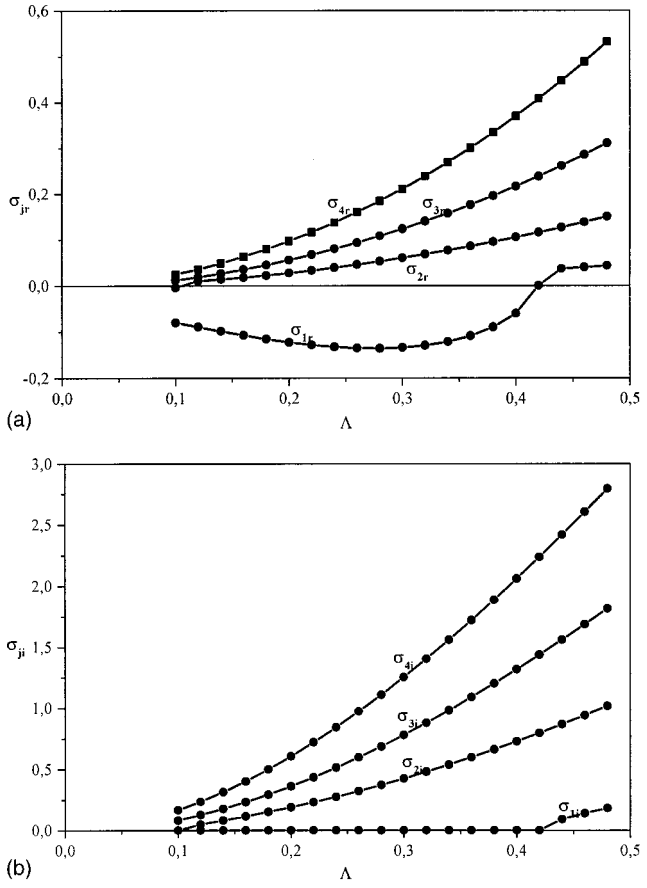

FIG. 7. Evolution of the (a) real and (b) imaginary part of the eigenvalues corresponding to the first four eigenmodes, $\sigma_{jr} j=1....4$, with increasing Λ; $C_{el}\epsilon=0.6$, $\epsilon=80$, $S=100$, Oh$=0.1$.

comes more intense as C_{el} increases. This effect is intensified when S drops below unity since the normal stress also becomes destabilizing in this case. The above set of eigenvalue calculations essentially verifies for leaky dielectrics the well known result for perfect dielectrics that both the critical wave number at which instability arises as well as the initial growth rate of the most unstable disturbance decrease as the intensity of the electric field increases (Nayyar and Murthy[27]). At the same time, however, it points out an important difference between leaky and perfect dielectric materials, which has also been confirmed experimentally,[18,19] namely that the application of the electric field can deteriorate bridge stability when $S<\epsilon$.

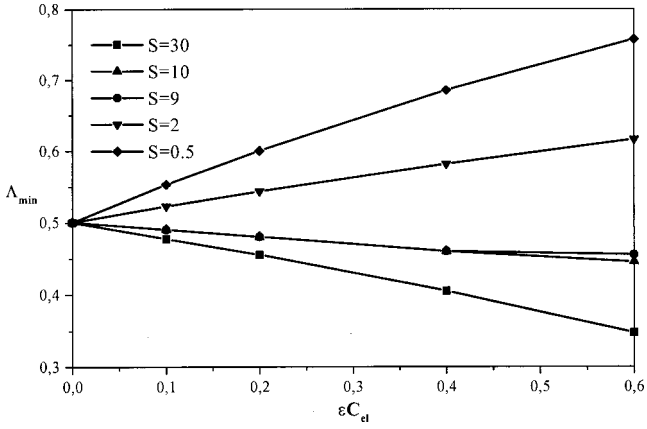

FIG. 8. Variation of the minimum aspect ratio, $\Lambda_{\min}$, for a cylindrical shaped bridge to be stable under varicose instabilities with increasing electric field intensity, $C_{el}\epsilon$, for different values of the conductivity ratio (a) $S=30$, (b) $S=10$, (c) $S=9$, (d) $S=2$, (e) $S=0.5$, $\epsilon=10$, Oh$=0.1$.

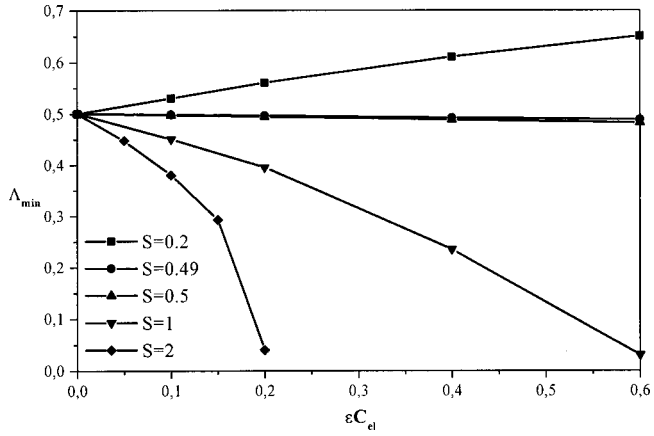

FIG. 9. Variation of the minimum bridge aspect ratio, $\Lambda_{\min}$, with increasing electric field intensity, $C_{el}\epsilon$, for different values of the conductivity ratio (a) $S=0.2$, (b) $S=0.49$, (c) $S=0.5$, (d) $S=1$, (e) $S=2$, $\epsilon=0.5$, Oh$=0.1$.

A similar set of numerical results is shown in Fig. 9 as S increases from 0.2 to 2 with ϵ set to 0.5 and Oh to 0.1. In this case, when S is much smaller than ϵ, the destabilizing effect of the tangential stress dominates over the stabilizing effect of the normal one and application of an electric field destabilizes the bridge. As S increases, somewhere in the interval 0.45 and 0.49, a critical value of S is attained beyond which the effect of the tangential stress dominates and the bridge is stabilized as ϵC_{el} increases. This behavior persists as S increases beyond 1. In fact when S becomes larger than, approximately, 10, the field tends to stabilize the entire range of aspect ratios Λ, something that was also observed by Saville[15] in the context of jet stability. A more specific comparison with analytical results[15] as well as with experimental observations[18,19] is given in the following paragraphs. An interesting aspect of the results presented in Figs. 8 and 9 is that the stability criteria obtained in the present study agree with those provided by the analysis of Saville.[15] This is due to the fact that the effect of S and ϵ on bridge stability is determined through the interfacial conditions governing the electric field, as will be demonstrated clearly in Sec. VI, which are common in Saville's analysis[15] and in the present study. It should also be noted that Oh does not affect the location of the bifurcation points signifying the transition from the cylindrical bridge to an amphora, or in other words the location of $\Lambda_{\min}$ which can also be obtained via static analysis as was seen for the case of perfect dielectrics.[16] Consequently, the stability characteristics of the bridge are qualitatively represented by the criteria presented in Ref. 15, however, the actual location of the bifurcation points, $\Lambda_{\min}$, is not necessarily the same as the one predicted in Ref. 15 since the latter study ignores the boundary layers near the two cylindrical rods supporting the bridge.

We now turn to the comparison of the predictions pro-

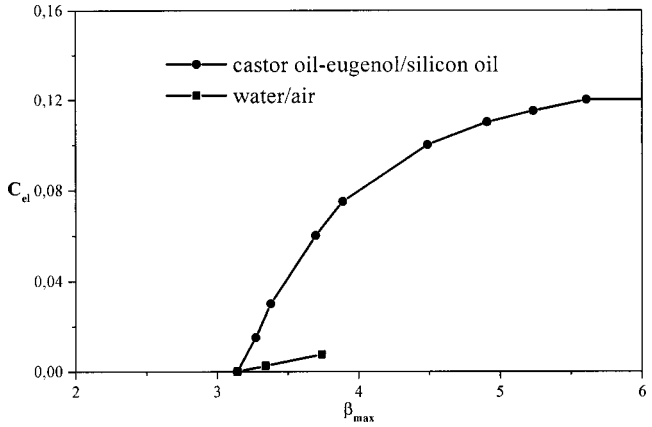

FIG. 10. Variation of the maximum slenderness ratio, $\beta_{\max}=\pi/2/\Lambda_{\min}$, with increasing electric field intensity, C_{el}, for a bridge with castor oil-eugenol and silicon oil occupying the inner and outer fluids, respectively ($S\to\infty$, $\epsilon=2.0$, Oh$=0.3$) and a water/air bridge ($S\to\infty$, $\epsilon=80.0$, Oh$=0.0025$).

vided by the model presented here with previous experimental investigations of liquid bridge stability. As was first observed experimentally by Sankaran and Saville[18] in terrestrial experiments, through the use of isopycnic systems, and subsequently verified by Burcham and Saville[19] aboard a space shuttle, by exchanging the inner and outer fluids of a bridge consisting originally of a castor oil-eugenol mixture and silicone, respectively, application of an electric field can destabilize the bridge. Thus when silicone is used as the inner fluid of the bridge the latter is destabilized when an electric field is applied. This result is a specific feature of the leaky dielectric model. In the same context it was concluded in Ref. 18 that bridge stability depends on the sign of the factor $(S-\epsilon)$. In order to test these results in the present study bridge stability is investigated for the castor oil-eugenol/silicon oil pair of inner and outer bridge fluids, respectively, in Fig. 10. Geometrical characteristics of the bridge as well as properties for the two materials are obtained from Ref. 18; $\tilde{R}=0.24\,\mathrm{cm}$, $\epsilon=2.0$, Re$=$Oh$^{-1}=0.3$, and $S\gg 1$. Due to the very large value of S and in order to avoid numerical error the case of $S\to\infty$ was examined numerically; more information on the modification of the numerical procedure in order to accommodate this limit is given in Sec. IV. In Fig. 10 C_{el} is plotted versus the maximum slenderness ratio $\beta_{\max}=\pi/(2\Lambda_{\min})$ in order to compare our results with the experimental observations of Sankaran and Saville[18] (Fig. 2 in their article). Clearly there is at least qualitative agreement between the two graphs. As $\beta_{\max}$ increases beyond the value obtained in the absence of an electric field, $\beta\approx 3.14$, there is an abrupt increase in the corresponding value of C_{el} until a plateau is reached. In this plateau even the slightest increase in the electric field strength results in a significant stabilization of the bridge, a behavior indicated by the experimental observations.[18,19] In fact when $C_{el}=0.15$ $\Lambda_{\min}\approx 0.03$ ($\beta_{\max}\approx 52$) which amounts to an almost complete stabilization of the bridge. It is interesting to note that Saville[15] in his analysis predicts that complete stabilization of a jet with $\epsilon=2$ and $S\to\infty$ is achieved when $C_{el}\approx 0.03(4\pi)=0.37$. Due to the increasing numerical errors as $\Lambda_{\min}$ decreases, we did not attempt to reproduce this prediction but the qualitative agreement between our approach and Saville's is obvious despite the fact that in the latter study a small Oh number was assumed for both the inner and the outer bridge fluids. The case of water/air ($\epsilon\approx 80$, Re$\approx$Oh$^{-1}\approx 400$, $S\to\infty$) was also examined numerically and it resulted in a much slower increase of β with increasing ϵC_{el} (Fig. 10); $0\leqslant\epsilon C_{el}\leqslant 0.6$. This is in agreement with the prediction by Saville[15] that when $\epsilon\approx 80$ the value of C_{el} that is required for complete stabilization of the bridge is $0.005(4\ \pi)=0.0628$ or, in terms of ϵC_{el}, 5. It should also be noted that application of the perfect dielectric model for the eugenol-castor oil/silicone oil and the water/air bridges predicts a much weaker stabilization of the bridge (larger $\Lambda_{\min}$) than the leaky dielectric model discussed above; for example, for eugenol-castor oil/silicone oil bridges application of the perfect dielectric model gives $\Lambda_{\min}\approx 0.49$ when $\epsilon C_{el}=0.6$. This also corroborates the proposition by Saville[15] that leaky dielectrics require a much lower field for their stabilization.

The pair silicone oil/castor oil-eugenol with silicone oil occupying the inner portion of the bridge is obtained by interchanging the inner and outer bridge fluids in the experimental setup described in the previous paragraph. This is a pair of fluids that is more compatible with the theory developed in the present study since the silicone oil used in Ref. 17 is much more viscous than castor oil. Hence, to a first approximation, viscous effects in castor oil can be neglected. Consequently, besides the bridge stability limit, $\Lambda_{\min}$, which does not depend on Oh, the damping or growth rates that are obtained for such a pair are expected to be more useful for a comparison against experimentally observed rates than the ones obtained for the case with silicon oil forming the outer bridge fluid. Using the physical constants provided by Sankaran and Saville[19] we obtain the following values for the dimensionless parameters of the silicon oil/castor oil eugenol bridge: $\epsilon=\epsilon_{\mathrm{in}}/\epsilon_{\mathrm{out}}=0.54$, $S=0.005$, Oh$=100$. For this set of parameter values and $\epsilon C_{el}=0.108$, $\Lambda_{\min}$ was calculated numerically to be 0.56. The experimentally measured value in Ref. 18 is $\tilde{L}/2\tilde{R}=2.05$, which becomes $\Lambda=0.76$ in terms of the definition for the aspect ratio adopted in the present study. Figure 11 shows the effect of varying field intensity C_{el} on $\Lambda_{\min}$ for a silicone bridge surrounded by a mixture of castor-oil and eugenol. Clearly, the bridge is destabilized as the intensity of the field is increased, a behavior that is observed in the experiments of Sankaran and Saville[18] and is compatible with the leaky dielectric model as opposed to the perfect dielectric model which does not predict bridge destabilization upon application of an electric field. The validity of the leaky dielectric model for the castor oil eugenol/silicon oil bridges was verified experimentally in the microgravity environment aboard a space shuttle[19] also. However, there are certain observations that do not conform with the leaky or the perfect dielectric models such as the inability of an ac field, oscillating at frequencies much higher than needed to nullify charge relaxation, to stabilize castor oil bridges in the dielectric gas sulphur hexafluoride,[19] SF_6, or the fact that the amphoras were always oriented with their bulge nearer the positive electrode[18] despite the fact that the

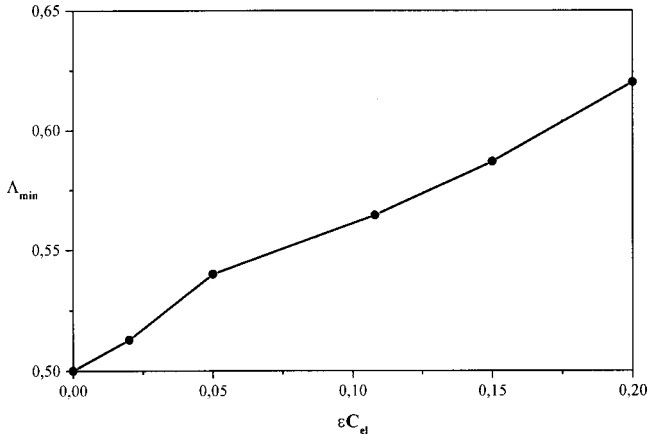

FIG. 11. Variation of the minimum bridge aspect ratio, $\Lambda_{\min}$, with increasing electric field intensity, ϵC_{el}, for a bridge with silicon oil and castor oil-eugenol occupying the inner and outer fluids, respectively; $S=0.005$, $\epsilon=0.54$, Oh$=100$.

bridge deformation scales with the square of the field strength and therefore the deformation should be independent of the field orientation. These are phenomena whose nature is not yet understood and require further investigation.

VI. INTERPRETATION OF RESULTS AND CONCLUDING REMARKS

As a means to obtain a better understanding of the pattern of behavior regarding the variation of $\Lambda_{\min}$ with the problem parameters we resort to the contribution of electric stresses to the momentum equation. Thus Eq. (49) yields the following form for the electric stresses contribution in the momentum balance, multiplied by (-1) in order to indicate a force acting on the bridge from the surrounding fluid,

$$
\begin{aligned}
&-\int_{-\pi/2}^{\pi/2}\Phi_i(-P_b+1)\Lambda\left(-\frac{\partial \overline{f}}{\partial z}\right)\underline{e}_z\,dz \\
&\quad-\int_{-\pi/2}^{\pi/2}\Phi_i C_{el}(\epsilon\underline{\overline{\tau}}_{elb}^{\text{in}}-\underline{\overline{\tau}}_{elb}^{\text{out}})|_{r=f_b}\cdot\Lambda\left(-\frac{\partial \overline{f}}{\partial z}\right)\underline{e}_z\,dz \\
&\quad-\int_{-\pi/2}^{\pi/2}\Phi_i C_{el}(\epsilon\underline{\overline{\tau}}_{el}^{\text{in}}-\underline{\overline{\tau}}_{el}^{\text{out}})|_{r=f_b}\cdot\underline{e}_r\,dz \\
&\quad=\int_{-\pi/2}^{\pi/2}\Phi_i C_{el}\left[\frac{\partial \overline{V}^{\text{in}}}{\partial z}(\epsilon-1)\underline{e}_r+(S-\epsilon)\right. \\
&\qquad\left.\times\left(\frac{1}{\Lambda}\frac{\partial \overline{V}^{\text{in}}}{\partial r}-\Lambda\frac{\partial \overline{f}}{\partial z}\right)\underline{e}_z\right]_{r=f_b}dz. \qquad (64)
\end{aligned}
$$

Closer examination of the right hand side of Eq. (64) reveals two different types of electric force. The first term represents the normal force exerted on the bridge due to the difference in permittivity constants between the two materials. The last term is always tangential to the interface, indicating a shear force, and is present only when leaky dielectrics are considered. The behavior of these terms depends solely on the solution of Laplace's equation in the two media subject to boundary condition (36) or (35), with the factor $(S-1)$ [see Eq. (36)] as a parameter for leaky dielectrics or the factor $(\epsilon-1)$ [see Eq. (35)] for perfect dielectrics, given the shape of the interface. First, the eigenvector corresponding to the first eigenmode, which is the most unstable one, is calculated and is normalized so that $\overline{f}(z)>0$ in the interval $0<z<\pi/2$, Figs. 12(a), 12(b). Figure 12(c) depicts the type of normal and tangential stress that act in a stabilizing or destabilizing fashion on the portion of the interface depicted in Figs. 12(a), 12(b). Examining the variation of the eigenvector along the interface $r=1$, it turns out that the tangential derivative

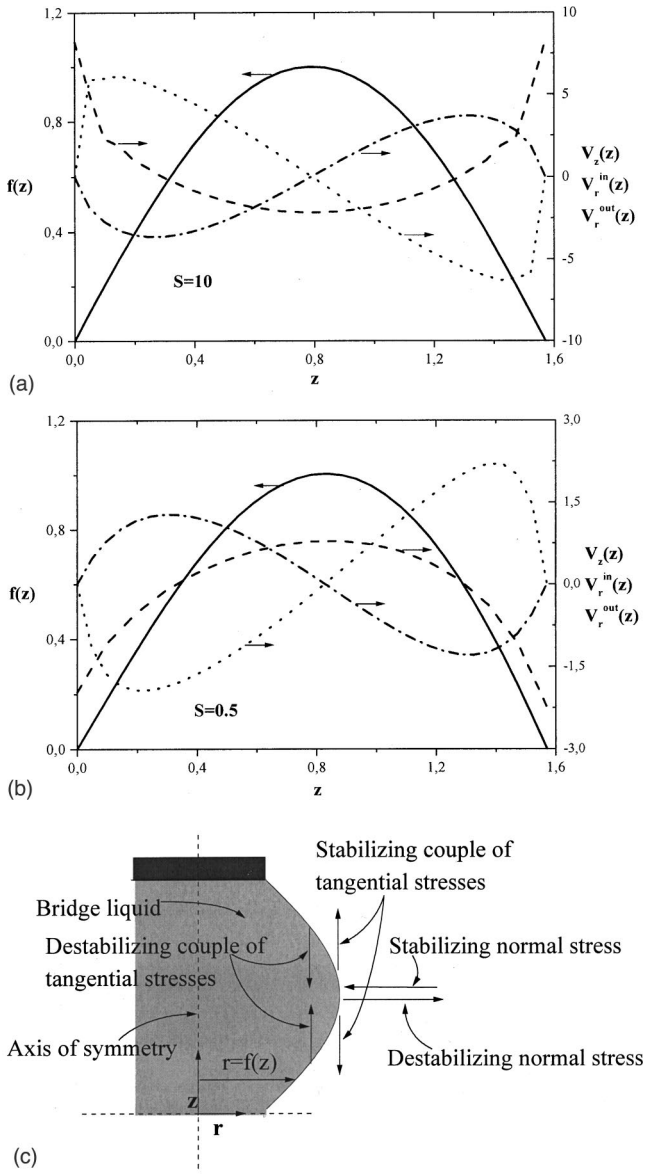

FIG. 12. Variation in the longitudinal direction, z, of $\overline{f}$, $\partial\overline{V}/\partial z$ — — —, $\partial\overline{V}^{\text{in}}/\partial r$ · · · ·, $\partial\overline{V}^{\text{out}}/\partial r$ —·—·—·—, as evaluated at the bridge interface for the eigenvector corresponding to the first mode: (a) $S=10$, (b) $S=0.5$, $\epsilon=80$, $\epsilon C_{el}=0.6$, Oh$=0.1$, $\Lambda=2$. (c) Schematic representation of the stabilizing or destabilizing normal and tangential forces acting on the upper half of a bridge whose interface is represented by the mode depicted in (a),(b).

TABLE I. Effect of electric properties of the inner and outer fluids on bridge stability. S_{crit} is a limiting value of S below which application of an electric field destabilizes the bridge. It depends on the specific values acquired by ϵ and C_{el}.

Normal electric stress $\sim(S-1)(\epsilon-1)$, $(S-1)(\epsilon-1)>0\rightarrow$Stabilization ($\Lambda_{min}<0.5$), $(S-1)(\epsilon-1)<0\rightarrow$Destabilization ($\Lambda_{min}>0.5$) Tangential electric stress $\sim(S-\epsilon)$ $(S-\epsilon)>0\rightarrow$Stabilization ($\Lambda_{min}<0.5$), $(S-\epsilon)<0\rightarrow$Destabilization ($\Lambda_{min}>0.5$)		
$\epsilon<1$	$\epsilon=1$	$\epsilon>1$
$S>1$ Tangential stress→Stabilizing Normal stress→Destabilizing Overall effect→Stabilizing	$S>\epsilon$ Tangential stress Stabilizing	$S>\epsilon$ Tangential stress→Stabilizing Normal stress→Stabilizing Over all effect→Stabilizing
$S=1$ Tangential stress→Stabilizing		$S=\epsilon$ (Perfect Dielectrics) Normal stress→Stabilizing
$\epsilon<S<1$ Tangential stress→Stabilizing Normal stress→Stabilizing Overall effect→Stabilizing	$S=\epsilon=1$ (same fluid) No effect	$1<S<\epsilon$ Tangential stress→Destabilizing Normal stress→Stabilizing $S<S_{Crit}$ Destabilization
$S=\epsilon$ (Perfect Dielectrics) Normal stress→Stabilizing		$S=1$ Tangential stress→Destabilizing
$S<\epsilon$ Tangential stress→Destabilizing Normal stress→Stabilizing $S<S_{Crit}$ Destabilization	$S<\epsilon$ Tangential stress Destabilizing	$S<1$ Tangential stress→Destabilizing Normal stress→Destabilizing Overall effect→Destabilizing

$$\frac{\partial \overline{V}^{in}}{\partial z}\left(=\frac{\partial \overline{V}^{out}}{\partial z}\right)$$

is negative around the interface crest when $S>1$, while the opposite is true when $S<1$. The normal derivative to the interface on the side of the bridge fluid, $(\partial \overline{V}^{in}/\partial r)$, changes sign from positive to negative as z increases around the crest of the interface when $S>1$, whereas the change in sign occurs in the opposite direction when $S<1$. The exact opposite is true for the normal derivative on the side of the fluid surrounding the bridge, $(\partial \overline{V}^{out}/\partial r)$. The same observations hold for the case of perfect dielectrics using ϵ instead of S. Finally, the derivative of the perturbation of the interface, $d\overline{f}/dz$, is positive before the crest turning negative as it crosses it approaching the fixed point attached to the upper rod.

In this fashion, examining the normal component of the stress in Eq. (64), which is the only remaining stress component in the case of perfect dielectrics, we can explain the findings of Gonzalez *et al.*[16] regarding the stability of an electric bridge when both fluids are treated as perfect dielectrics. More specifically, the tangential derivative of the electric potential around the crest of the interface behaves like $-(\epsilon-1)$, or $-(S-1)$ for leaky dielectrics, and consequently its contribution to the force on the interface due to the normal stress component is like $-(\epsilon-1)^2$, or like $-(S-1)(\epsilon-1)$ for leaky dielectrics. In fact, it will always be negative for perfect dielectrics, tending to eliminate the crest of the interface thus stabilizing the bridge and maintaining Λ_{min} below 0.5, as predicted in Ref. 16. In the case of leaky dielectrics the action of this term will depend on the relative magnitude of S and ϵ with respect to unity, as was pointed out by Saville.[15]

When leaky dielectrics are considered the tangential stress component enters the force balance in Eq. (64). The term $-(d\overline{f}/dz)$ acquires negative and positive values around the location of maximum displacement of the interface in such a way that, when $S>\epsilon$, the shear forces corresponding to this term on either side of the crest point away from it tending to eliminate large displacements and stabilizing the bridge. In the same fashion this term has a destabilizing effect when $S<\epsilon$. The same argument is true for the normal derivative of the electric potential evaluated on the side of the bridge fluid, $\partial \overline{V}^{in}/\partial r$, when $S<1$. Namely, the stabilizing or destabilizing action of the latter term depends on the factor $(S-\epsilon)$ with a positive value indicating stabilization. Turning to the case with $S>1$, in order to determine its effect on bridge stability we first employ interfacial condition (36) according to which the term multiplying $(S-\epsilon)$ in Eq. (64) is equal to

$$\left(\frac{1}{\Lambda}\frac{\partial \overline{V}^{out}}{\partial r}-\Lambda\frac{\partial \overline{f}}{\partial z}\right)\frac{1}{S}.$$

When $S>1$ the normal derivative of the electric potential, evaluated on the side of the outer bridge fluid, crosses zero to positive values around the interface crest in such a way as to result in a shear force that, for positive $S-\epsilon$, points away from the crest stabilizing the bridge. Consequently, for the entire range of values of S (below or above unity) the action of the shear force on the interface is determined by the factor

$(S-\epsilon)$, a feature first pointed out in Ref. 15, with positive values indicating stability and $\Lambda_{\min}$ remaining below 0.5 while the opposite is true when $S<\epsilon$.

Concluding, it should be pointed out that the linear stability of a liquid bridge was examined upon application of an axial electric field treating the bridge fluids as leaky dielectrics, and the effect of the latter was identified as stabilizing when $S \geqslant \epsilon$, in the sense that the minimum value of the bridge aspect ratio, $\Lambda_{\min}$, was seen to decrease below 0.5 (the critical minimum value for stability obtained in the absence of the electric field), as the intensity of the electric field increases (C_{el} increases). When $S<\epsilon$ there is a critical value of S below which the electric field actually destabilizes the bridge constantly increasing $\Lambda_{\min}$ above 0.5 as C_{el} increases. This type of behavior is a result of the combined action of the normal and tangential electric stress components on the perturbed interface whose action is determined by factors $(S-1)(\epsilon-1)$ and $(S-\epsilon)$, respectively. When perfect dielectrics are considered the contribution of the tangential stress component vanishes and the electric field has invariably a stabilizing effect on the bridge. These stability conditions do not depend on Oh as they identify bifurcation points marking the transition from a perfect cylindrical bridge to an amphora shape. They were first proposed by Saville,[15] in his analytical study on the stability of cylindrical jets under the action of a longitudinal electric field, confirmed numerically for the case of perfect dielectrics via a static analysis[16] and, partly, verified experimentally in terrestrial[18] and microgravity[19] experiments. A systematic tabulation of the stability criteria for perfect and leaky dielectrics is provided in Table I.

Finally, increasing the intensity of the electric field, as it is measured by C_{el}, only intensifies the above behavior tending to stabilize the entire range of bridge aspect ratios when it becomes large enough, provided we operate in the parameter range for which application of an electric field stabilizes the bridge. Under these conditions extremely long bridges may be generated, as was experimentally observed by previous investigators.[9,10] Therefore, an electric field can stabilize a liquid bridge much more effectively than can a shear flow field, applied on its outer surface.[28] In a future study it will be interesting to follow Chen and Tsamopoulos[29] and include the effects of gravity, external fluid viscosity, and nonlinearity in the analysis, thus allowing for better simulation of the available experimental investigations and complete coverage of the relevant parameter range. Finally, it would be very interesting to examine break-up of the bridge and formation of drops as in Zhang and Basaran,[30] Zhang *et al.*[31] and Ramos *et al.*[32]

ACKNOWLEDGMENTS

This work was partially supported under the EPEAEK program (Grant No. 51) of the Ministry of Education of Greece. The authors wish to acknowledge the help of S. Dragoumanos in conducting some of the numerical tests that were used for verifying the validity of the numerical method. The authors also wish to thank an anonymous referee for his/her insightful and helpful comments.

[1] R. Brown, "Theory of transport processes in single crystal growth from the melt," AIChE J. **34**, 881 (1988).
[2] J. S. Finucane and D. R. Olander, "The viscosity of uranium–chromium alloys," High. Temp. Sci. **1**, 466 (1969).
[3] J. M. Lihrmann and J. S. Haggerty, "Surface tensions of alumina-containing liquids," J. Am. Chem. Soc. **68**, 81 (1985).
[4] G. H. McKinley and A. Tripathi, "How to extract the Newtonian viscosity from capillary breakup measurements in a filament rheometer," J. Rheol. **44**, 653 (2000).
[5] J. Plateau, "Experiments and theoretical researches on the figures of equilibrium of a liquid mass withdrawn from the action of gravity, etc.," *Annual Reports of the Board of Regents of the Smithsonian Institution*.: Pt. 1, House of Representatives Misc. Doc. #83, 38th Congress, 1st Session, pp. 207–277; Pts. 2–4, Misc. Doc. #54, 38th Congress, 2nd Session, pp. 285–369; Pt. 5, Misc. Doc. #102, 39th Congress, 2nd Session, pp. 411–435; Pt. 6, Misc. Doc. #83, 39th Congress, 2nd Session, pp. 255–289 (1863–1866).
[6] Lord Rayleigh, "On the instability of jets," Proc. London Math. Soc. **10**, 4 (1879).
[7] S. R. Coriell, S. C. Hardy, and M. R. Cordes, "Stability of liquid zones," J. Colloid Interface Sci. **60**, 126 (1977).
[8] J. A. Tsamopoulos, T. Y. Chen, and A. Borkar, "Viscous oscillations of capillary bridges," J. Fluid Mech. **235**, 579 (1992).
[9] R. J. Raco, "Electrically supported column of liquid," Science **160**, 311 (1968).
[10] G. I. Taylor, "Electrically driven jets," Proc. R. Soc. London, Ser. A **313**, 453 (1969).
[11] J. R. Melcher and G. I. Taylor, in *Annual Review of Fluid Mechanics*, edited by W. R. Sears and M. Van Dyke (Annual Reviews, Palo Alto, CA, 1969), pp. 111–146.
[12] R. S. Allan and S. G. Mason, "Particle behavior in shear and electric fields, I. Deformation and burst of liquid drops," Proc. R. Soc. London, Ser. A **267**, 45 (1962).
[13] G. I. Taylor, "Studies in electrohydrodynamics. I. The circulation produced in a drop by an electric field," Proc. R. Soc. London, Ser. A **291**, 159 (1966).
[14] J. A. Tsamopoulos, T. R. Akylas, and R. A. Brown, "Dynamics of charged drop breakup," Proc. R. Soc. London, Ser. A **401**, 67 (1985).
[15] D. A. Saville, "Electrohydrodynamic stability: Fluid cylinders in longitudinal electric fields," Phys. Fluids **13**, 2987 (1970).
[16] H. Gonzalez, F. M. J. McCluskey, A. Castellanos, and A. Barrero, "Stabilization of dielectric liquid bridges by electric fields in the absence of gravity," J. Fluid Mech. **206**, 545 (1989).
[17] A. Ramos, H. Gonzalez, and A. Castellanos, "Experiments of dielectric liquid bridges subjected to axial electric fields," Phys. Fluids **6**, 3206 (1994).
[18] S. Sankaran and D. A. Saville, "Experiments on the stability of a liquid bridge in an axial electric field," Phys. Fluids A **5**, 1081 (1993).
[19] C. L. Burcham and D. A. Saville, "The electrohydrodynamic stability of a liquid bridge: Microgravity experiments on a bridge suspended in a dielectric gas," J. Fluid Mech. **405**, 37 (2000).
[20] D. A. Saville, "Electrohydrodynamics: The Taylor–Melcher leaky dielectric model," Annu. Rev. Fluid Mech. **29**, 27 (1997).
[21] J. A. Stratton, *Electrodynamic Theory* (McGraw-Hill, New York, 1941).
[22] T. B. Benjamin and J. C. Scott, "Gravity-capillary waves with edge constraints," J. Fluid Mech. **92**, 241 (1979).
[23] R. B. Lehoucq and J. A. Scott, "An evaluation of software for computing eigenvalues of sparse nonsymmetric matrixes," MCS-P547-1195, Argonne National Laboratory (1996).
[24] A. Borkar and J. A. Tsamopoulos, "Boundary-layer analysis of the dynamics of axisymmetric capillary bridges," Phys. Fluids A **3**, 2866 (1991).
[25] A. Sanz and J. L. Diez, "Nonaxisymmetric oscillation of liquid bridges," J. Fluid Mech. **205**, 503 (1989).
[26] M. Strani and F. Sabetta, "Viscous oscillations of a supported drop in an immiscible fluid," J. Fluid Mech. **189**, 397 (1988).
[27] N. K. Nayyar and G. S. Murty, "The stability of a dielectric liquid jet in the presence of a longitudinal electric field," Proc. Phys. Soc. London **75**, 369 (1960).

[28]B. J. Lowry and P. H. Steen, ''Stability of slender liquid bridges subjected to axial flows,'' J. Fluid Mech. **330**, 189 (1997).
[29]T. Y. Chen and J. A. Tsamopoulos, ''Nonlinear dynamics of capillary bridges: Theory,'' J. Fluid Mech. **255**, 373 (1993).
[30]X. Zhang and O. A. Basaran, ''Dynamics of drop formation from a capillary in the presence of an electric field,'' J. Fluid Mech. **326**, 239 (1996).
[31]X. Zhang, R. S. Padgett, and O. A. Basaran, ''Nonlinear deformation and break-up of stretching liquid bridges,'' J. Fluid Mech. **329**, 207 (1996).
[32]A. Ramos, F. J. Garcia, and J. M. Valverde, ''On the breakup of slender liquid bridges: Experiments and 1-D numerical analysis,'' Eur. J. Mech. B/Fluids **18**, 649 (1999).